The tardigrade *Hypsibius exemplaris* dramatically upregulates DNA repair pathway genes in response to ionizing radiation

Courtney M. Clark-Hachtel[1,2,6,7,8,*], Jonathan D. Hibshman[1], Tristan De Buysscher[1,3], Evan R. Stair[4], Leslie M. Hicks[4], and Bob Goldstein[1,5]

[1] Biology Department, The University of North Carolina at Chapel Hill, Chapel Hill, NC 27599, USA

[2] Biology Department, The University of North Carolina at Asheville, Asheville, NC 28804, USA

[3] Bioinformatics & Analytics Research Collaborative, The University of North Carolina at Chapel Hill, Chapel Hill, NC 27599, USA

[4] Department of Chemistry, University of North Carolina at Chapel Hill, Chapel Hill, NC 27599, USA

[5] Lineberger Comprehensive Cancer Center, The University of North Carolina at Chapel Hill, Biology, Chapel Hill, NC 27599, USA

[6] Current Address: Biology Department, The University of North Carolina at Asheville, Asheville, NC 28804, USA

[7] X (formerly Twitter): ArthropodQueen

[8] Lead contact

*Correspondence: clarkcm6@email.unc.edu

KEYWORDS: tardigrades, radiation tolerance, DNA repair, genome stability

SUMMARY

Tardigrades can survive remarkable doses of ionizing radiation, up to about 1000 times the lethal dose for humans. How they do so is incompletely understood. We found that the tardigrade *Hypsibius exemplaris* suffers DNA damage upon gamma irradiation, but damage is repaired. We show that this species has a specific and robust response to ionizing radiation: irradiation induces a rapid upregulation of many DNA repair genes. This upregulation is unexpectedly extreme – making some DNA repair transcripts among the most abundant transcripts in the animal. By expressing tardigrade genes in bacteria, we validate that increased expression of some repair genes can suffice to increase radiation tolerance. We show that at least one such gene is important *in vivo* for tardigrade radiation tolerance. We hypothesize that tardigrades' ability to sense ionizing radiation and massively upregulate specific DNA repair pathway genes may represent an evolved solution for maintaining DNA integrity.

INTRODUCTION

Some organisms have evolved to survive conditions that to most organisms would be lethal, including extreme heat, extreme cold, and desiccation[1–7]. Revealing the mechanisms that these organisms employ to survive under stressful conditions can aid in understanding stress tolerance and may contribute to improving the survival of less tolerant organisms, cells, or biological materials in the face of stress.

Tardigrades are well known for their ability to survive in environments where other animals would not[5,6]. Some tardigrade species have been demonstrated to survive desiccation as well as extreme pressures, low temperatures, and high levels of ionizing radiation (IR)[5–11]. For example, while the dose of IR at which 50% of humans would die (LD50) is 5 gray (Gy), the tardigrade *Hypsibius exemplaris* can survive ~4,000 Gy[12,13]. At these levels of IR we would expect massive amounts of DNA damage and genomic instability[14,15].

Little is known about the specific mechanisms that underlie tardigrade extreme resistance to genotoxic stress. Most of what is known comes from work in the tardigrade *Ramazzottius* cf. *varieornatus*, a species with a similar IR tolerance to *H. exemplaris*[15]. *R.* cf. *varieornatus* produces a DNA damage suppressing protein (Dsup) that can confer IR resistance when expressed in human cultured HEK 293T cells[15,16]. Biochemical studies of this protein have revealed that it protects DNA from IR by binding to DNA and nucleosomes and protecting DNA from hydroxyl radicals that are generated by IR-exposed cells[17]. The identification of Dsup suggested that *R.* cf. *varieornatus* can survive high doses of IR through the employment of

protective mechanisms that prevent damage to the DNA. However, it remains unclear if protective mechanisms can fully explain the extreme IR tolerance of tardigrades. The protein sequence of Dsup is not well conserved within the eutardigrade lineage; hence, it is unclear if other eutardigrade species' Dsup proteins have the same protective abilities[16,18]. Furthermore, heterotardigrade species, some of which have been shown to have strong IR tolerance, seemingly lack a Dsup homolog, suggesting that different tardigrade species may employ different mechanisms to survive high levels of IR[18–20].

Here, we set out to understand how the tardigrade *H. exemplaris* can survive extreme IR. Through DNA damage assays, expression analyses, and functional studies, we show that *H. exemplaris* tardigrades do experience DNA damage upon IR exposure, that they upregulate DNA repair transcripts to a remarkable and unexpected degree in response to IR, and that the increased expression of some DNA repair transcripts is both sufficient to confer IR tolerance to bacteria and important for *H. exemplaris* IR tolerance.

RESULTS

H. exemplaris *experiences DNA damage from ionizing radiation*

To visualize the level and location of DNA damage in tardigrades following IR exposure, we adapted a terminal deoxynucleotidyl transferase dUTP nick end labeling (TUNEL) assay for use on whole animals (see STAR Methods). TUNEL assays are commonly used to visualize DNA single-stranded (ss) and double-stranded (ds) breaks [21]. We exposed animals to a well-tolerated dose of gamma irradiation (2,180 Gy), as well as a dose near the LD50 (4,360 Gy)[13]. Animals that were never exposed to IR had little TUNEL signal throughout their nuclei (Figure 1). We found that animals exposed to IR had significantly more TUNEL signal per nucleus than control animals (Figure 1). This suggests that the tardigrades indeed experience DNA damage from IR exposure. To determine if damage is repaired, we exposed animals to the same doses of gamma irradiation and allowed them to recover for 24 hours (Figure 1). After a sub-lethal irradiation dose, animals that were exposed to IR and allowed to recover showed a significant reduction in TUNEL signal per nucleus over 24 hours of recovery (Figure 1D). These results suggest that *H. exemplaris* experiences DNA damage upon extreme levels of IR but is then able to repair much of the damage.

H. exemplaris *upregulates the transcription of DNA repair pathway genes after exposure to ionizing radiation or the DNA-damaging agent bleomycin*

H. exemplaris could be engaging in a variety of measures to compensate for DNA damage, including transcriptomic responses. The well-established animal DNA damage response only minimally involves transcriptional responses[22], yet some modest transcriptional responses to DNA damaging agents have been observed in other animals with a typical enrichment of 1.5-4 fold for any responsive transcript[23–29]. *H. exemplaris* specifically has robust transcriptional responses to desiccation, a stress that can also result in DNA damage[30–33]. To examine tardigrade transcriptomes after IR, we performed messenger RNA sequencing (mRNA-Seq) on animals after exposure to 100, 500, or 2,180 Gy doses of IR. *H. exemplaris* can survive and reproduce after exposure to 100 Gy[13]. After exposure to 500 or 2,000 Gy (about half of the LD50), they survive well but no longer reproduce[13].

Differential expression analysis revealed that *H. exemplaris* has a robust transcriptional response to IR exposure, with 4,590 transcripts significantly upregulated and 4,687 downregulated in response to 500 Gy IR ($p<.05$, Figure 2A, Data S1B)**.** We were intrigued to find that 7 of the top 15 most significantly enriched transcripts encoded proteins of DNA repair pathways (Figure 2A, Table S1). These transcripts included representatives from Base Excision Repair (BER) (*DNA LIG1*, *PNKP*, *PARP3*, *PARP2*, and *PCNA*) and Non-Homologous End Joining (NHEJ) (*XRCC5*, which encodes Ku80, and *DNA LIG4*) (Figure 2A, Table S1), all of which were upregulated more than 32-fold (Table S1). By comparison, a recent study of the transcriptional response to IR in mammalian cells (X-ray, 2 Gy) identified only *PCNA* and *LIG1* from this list, both of which were upregulated less than 2-fold[24]. The remaining genes from the top 15 list are predicted to encode two eutardigrade-specific proteins with no conserved domains, two predicted histone proteins, a mitochondrial chaperone BCS1, a protein phosphatase 1B, a protein with RING-HC and WWE domains, and a partial Ku70 protein with no predicted DNA repair function (see STAR Methods[34]) (Table S1). The fact that multiple DNA repair pathway transcripts are represented in the most significantly enriched transcripts indicates that *H. exemplaris* responds to the damage caused by IR by upregulating genes encoding proteins that can correct damage. The degree of upregulation after IR was high (Log_2FC ranging from 5.38-8.30, i.e. 32- to 315-fold, Table S1). In addition, DNA repair genes constituted some of the most highly represented transcripts in the animals' transcriptome after IR (Figure 2B-D and Table S1 and S2) bringing some DNA repair transcripts up nearly to the level of highly expressed housekeeping genes like elongation factor 1-alpha and cytoplasmic actin (determined by TPM, Table S2). We performed a gene ontology (GO) analysis for the top 500 most significantly enriched genes following 500 Gy IR. Out of the genes that mapped to GO terms, 8.6% and 2.3% were assigned to "DNA binding" and "DNA repair", respectively (Data

S1B). The repair pathways that were most represented after IR exposure (NHEJ and BER) are most apt to repair the types of DNA damage that commonly result from exposure to IR[35]. IR can directly generate dsDNA breaks, which are repaired primarily by the NHEJ pathway[35,36]. IR exposure can also lead to the production of reactive oxygen species, which can cause ssDNA breaks as well as damaged bases, both of which are repaired by BER[35,37].

We were curious if other transcripts from NHEJ and BER pathways or from other DNA repair pathways were also enriched after exposure to IR. We found that multiple BER pathway genes were indeed enriched following IR exposure (Figure 2B, Table S1 and S3). In addition to the BER genes listed above, the scaffolding protein *XRCC1* was also enriched. We conclude that many of the genes important for BER are upregulated in response to IR. From NHEJ, *XRCC6* (which encodes Ku70) was also enriched following IR (Figure 2C, Table S3) which, in combination with XRCC5 and *LIG4* mentioned above, forms a complete set of the minimal proteins sufficient to perform NHEJ repair *in vitro*[38].

To examine whether *H. exemplaris* upregulates other DNA repair pathways in response to IR, we also looked at transcript enrichment for genes from the Mismatch Repair (MMR, repairs base mismatches), Nucleotide Excision Repair (NER, removes bulky adducts), Homologous Recombination (HR, repairs dsDNA breaks), and Theta-Mediated End Joining (TMEJ, repairs dsDNA breaks) pathways[35,39,40]. Amongst HR-associated genes, *RAD51* and *BARD1-like* were enriched following IR (Figure 2D, Table S3). Transcripts encoding two out of the three homologs for TMEJ proteins that we identified in tardigrades (DNA polymerase Theta (POLQ) and LIG1) were also significantly enriched following IR (Figure 2D, Table S1 and S3). No genes from NER or MMR pathways had transcripts significantly enriched following IR (Figure 2D, Table S4). Taken together, these results reveal specificity in the transcriptional response of *H. exemplaris* to IR, with animals increasing the expression of DNA repair genes from pathways that deal with the types of damage expected to result from IR. Two of these DNA repair pathways are associated with error-prone repair (NHEJ and TMEJ)[41]. The strong enrichment of transcripts that encode members of these pathways following IR suggests that even error-prone repair may contribute to *H. exemplaris* IR tolerance. We found that many of these DNA repair genes are strongly upregulated even after a 100 Gy dose over one hour (Figure 2E and Data S1B), suggesting a rapid and robust response. Additionally, many of these genes remained enriched after a 2,180 Gy dose incurred over approximately 24 hours, suggesting that the initial robust response is sustained for some time (Figure 2E and Data S1B).

We were curious if the enrichment of the transcripts that encode DNA repair proteins would result in an increase in protein levels as well. Using label-free quantitative proteomics, we were able to quantify six of the DNA repair proteins of interest after exposure to 500 Gy IR and a recovery period of either 6 or 18 hours (PNKP, PCNA, PARP3, BARD1-like, XRCC5, and XRCC6, Figure 2F). Although not significantly increased at a threshold FDR<0.05, $Log_2FC>1$, the relative abundance of most of the DNA repair proteins identified trends upwards 18 hours after exposure to IR, with four proteins having $Log_2FC > 1$ and FDR < 0.10 across the untreated and 18-hour recovery conditions. It has been recently observed using an isobaric labeling method and further verified through Western blots that the majority of these DNA repair proteins are significantly enriched at 24 hours after exposure to 1000 Gy IR, including XRCC5, which was the only repair protein that had a modest downward trend in our analysis[42]. Taken together, this suggests that DNA repair components are also enriched at the protein level following IR exposure.

Like IR, desiccation is also a stress that results in DNA damage[43,44]. Some similarities in transcriptomic responses to desiccation and other DNA damaging agents such as UV radiation have been previously reported for tardigrades[45]. We were curious if we would see a correlation between the transcriptomic responses of tardigrades to desiccation and those of IR. Comparing the changes in relative abundance of each transcript in response to desiccation vs IR did not reveal an obvious correlation in the transcriptional responses to these two stresses (Figure 3A-B)[30–32]. This result suggests that, at least at the transcriptional level, *H. exemplaris* may employ different methods to deal with these two genotoxic stressors.

As mentioned, IR creates dsDNA and ssDNA breaks and can result in damaged DNA bases through the action of ROS[35–37]. It is possible that the transcriptomic responses we observed are triggered by mechanisms linked to DNA damage. However, it is also possible that the production of ROS induced by IR leads to oxidative stress and this signal is responsible for activating the transcriptomic response to IR. To test if DNA damage induces the transcriptomic responses we observed regardless of the cause of damage, we induced DNA damage in *H. exemplaris* by soaking them in the chemotherapy drug bleomycin. Bleomycin is a known radiomimetic and induces both ssDNA and dsDNA breaks[46]. From the doses that we performed survival analyses on, we identified that a treatment of 1 mg/mL bleomycin for 24 hours is physiologically similar to a 500 Gy IR treatment in that animals survive the treatment but are no longer able to reproduce (11.7% survival 7 days after bleomycin treatment, Figure S1 A and B)[13]. We performed mRNA sequencing on animals exposed to 10 µg/mL, 100 µg/mL, and 1 mg/mL bleomycin and compared the transcriptomic response to what we observed from our 500

Gy IR treatment. We found evidence for a correlation between the transcriptional responses to these two genotoxic stresses, with all the DNA repair transcripts that are significantly enriched by IR also significantly enriched by each concentration of bleomycin examined (Figure 3C, Figure S1 C and D, Pearson correlation test $p<0.0001$, $r^2=0.0962$, 0.2311, and 0.2103 for 10 µg/mL, 100 µg/mL, and 1 mg/mL respectively). This outcome supports the idea that *H. exemplaris* may be responding specifically to the DNA damage that IR induces and validates bleomycin as a radiomimetic tool for this species. It is worth noting here that homologs of some of the transcripts induced by IR in *H. exemplaris* are also modestly induced by UV radiation in *R.* cf. *varieornatus* (transcripts encoding Ku80, PARP2*,* histone H4 domain-containing protein, core histone macro-H2A.1, and mitochondrial chaperone BCS1)[45]. Although UV irradiation and IR initially create fundamentally different types of DNA damage (bulky adducts vs. ssDNA and dsDNA breaks, respectively)[35–37,47], their resolution can utilize both BER and dsDNA repair pathways[47], lending further support to the idea that these animals are sensing the specific type of DNA damage and responding accordingly.

DNA repair transcripts are upregulated throughout the animal following ionizing radiation exposure with some tissue-specific enrichment

Our results above, demonstrating a strong and diverse response to IR, led us to wonder whether these responses occur throughout entire tardigrades or whether there are specific tissues that drive this response. To determine whether specific tissues respond to IR by upregulating repair transcripts, we performed *in situ* hybridization for a sample of the DNA repair transcripts that were enriched following IR exposure. After exposure to 100 Gy IR, enrichment of transcripts was detectable via *in situ* hybridization for the DNA repair transcripts that we examined, confirming our mRNA-Seq results (Figure 4, Figure S2-S4). All DNA repair transcripts that we observed became enriched in nearly all examined tissues after IR exposure (Figure S4) but also demonstrated some extent of tissue-specific enrichment (Figure 4, Figure S2-S4). For multiple DNA repair genes, transcripts were especially enriched in cuticle-forming tissues (stylet glands, claw glands, and the hindgut) (Figure 4, Figure S2-S4)[48,49]. In addition, we observed expression enrichment in storage cells (coelomocytes) for all but one of the DNA repair transcripts we observed (Figure S4). We conclude that the responses to IR exposure that we have identified are strongest in certain tissues, including cuticle-forming tissues, which are expected to be especially active in transcription and translation.

Expression of tardigrade DNA repair transcripts in bacteria can confer resistance to ionizing radiation

We considered it likely that the increased expression of DNA repair transcripts that we found in *H. exemplaris* might be sufficient to protect against IR exposure. Gene editing technology is in its infancy in tardigrades, making sufficiency experiments within *H. exemplaris* difficult[50]. To validate whether increased expression of these transcripts can ever suffice to increase protection against IR, we instead expressed tardigrade DNA repair genes heterologously in *Escherichia coli* (*E. coli*), a biologically simple system for evaluation of IR tolerance phenotypes. Bacteria induced to express *H. exemplaris* DNA repair genes were exposed to 2,180 Gy IR to see if they would survive better than *E. coli* containing control expression vectors that were either empty (no gene insertion) or contained a control sequence encoding GFP. In addition, we used a vector expressing the *R.* cf. *varieornatus Dsup* gene as a positive control, as it has been previously shown to improve radiation survival of human HEK 293T cells[15]. We found that expression of some tardigrade DNA repair genes could significantly improve the IR tolerance of *E. coli* relative to controls (Figure 5A and Figure S5). Transcripts that improved survival included *RAD51*, *XRCC1*, *FEN1*, *LIG1, PARP2,* and *POLB*. All of these genes except for *RAD51* (HR pathway) encode proteins in the BER pathway (Figure 5A). For some DNA repair genes, expression conferred about as strong protection as did expression of the known DNA protectant Dsup (Figure 5A). This improved survival is not caused simply by induction of transcription per se, as the bacteria carrying the control vectors were also transcriptionally induced. Many of the *H. exemplaris* DNA repair components that confer IR tolerance to *E. coli* do not have homologs in bacteria[35]. The few that do include *RAD51* (RecA) and *LIG1* (bacterial DNA ligase)[35]. *RAD51* encodes a DNA-binding protein and may provide IR protection in a heterologous system via physical interaction with DNA[51]. Due to its homology to RecA, RAD51 could also be hardening bacteria to IR through activation of the bacterial DNA damage response[52]. The conservation of *LIG1* from bacteria through humans presents the possibility that this DNA repair component may be improving IR survival in *E. coli* through its ligase activity, although further work needs to be done to confirm this. Some of the *H. exemplaris* DNA repair components that result in improved IR survival of *E. coli* have evolved to function in multi-protein complexes that bacteria lack[35] and thus may protect bacteria from IR by different mechanisms than those used in *H. exemplaris*. Regardless of the specific mechanisms of protection, these data validate the expectation that increased expression of these transcripts in an organism can indeed be sufficient to confer increased protection against IR.

A ***DNA repair transcript is required for*** **H. exemplaris** ***ionizing radiation tolerance***

To determine if one of the upregulated DNA repair transcripts is essential for the ability of tardigrades to survive IR, we attempted to decrease the amount that a DNA repair transcript

enriches in response to IR via RNA interference (RNAi). *H. exemplaris* is amenable to RNAi and has a systemic RNAi response: genes can be targeted in adults and their offspring by injection of double-stranded RNA (dsRNA) into individual animals[30,53]. We chose *XRCC5* as a target because it was among the most significantly enriched gene transcripts following exposure to IR (Figure 2A and C, Table S1 and S2) and because its importance to IR tolerance in mammals has been previously shown[54]. Although expression of *XRCC5* in *E. coli* did not enhance IR tolerance, this is likely an issue with solubility of the heterologously expressed protein[55] and not reflective of the importance of *XRCC5* to *H. exemplaris* IR tolerance (Figure S5). Most animals that were injected with dsRNA targeting either *XRCC5* or the control gene *GFP* survived over a 7-day period in the absence of IR exposure (Figure 6). After exposure to IR, animals that were injected with dsRNA targeting *XRCC5* had reduced survival compared to the *GFP*-targeted controls (Figure 6). We conclude that the high levels of *XRCC5* transcripts that we found in tardigrades after exposure to IR contribute to the animals' ability to survive this stress. This result suggests that at least one of the genes we identified as strongly upregulated (enriched 315-fold, $Log_2FC=8.3$) following IR plays a functional role in surviving IR exposure.

DISCUSSION

We found that the tardigrade *H. exemplaris* experiences DNA damage upon extreme doses of IR, and that they can repair much of that damage. This is in line with other studies that have either suggested or found evidence for DNA repair having a role in tardigrade survival following other stresses, including desiccation and UV irradiation[18,44,45,56,57]. Our mRNA-Seq analysis revealed an unexpectedly strong upregulation of DNA repair pathway genes in response to IR, with some transcripts enriched close to 300-fold, becoming among the most-represented transcripts in the animal's transcriptome. The repair pathways that were most affected are those most clearly implicated in repairing the types of DNA damage that would be expected following IR exposure: BER, which repairs oxidative damage and ssDNA breaks, and NHEJ, which repairs dsDNA breaks. The specificity and magnitude of this transcriptional response, along with the correlation of this response to that of bleomycin treatment, suggests that *H. exemplaris* has mechanisms for sensing the DNA damage caused by IR and in response, strongly increases the expression of specific DNA repair pathway genes. We found that RNAi targeting one such gene compromised the tardigrades' ability to survive high doses of IR. We also found that strong expression of some of these DNA repair transcripts alone is sufficient to confer IR tolerance to bacteria. We conclude that *H. exemplaris* has an adaptive response to DNA damage-inducing

radiation that is unique to date: they survive the damage at least in part by massive transcriptional upregulation of DNA repair pathway genes. Taken together, these results expand our understanding of the mechanisms that animals use to maintain DNA integrity under damaging conditions and may provide potential new routes forward to improving DNA stability in other systems.

Why tardigrades have evolved strong IR tolerance is enigmatic, given that it is unlikely that tardigrades were exposed to high doses of IR in their evolutionary history. One possible explanation for their exceptional IR tolerance is that their adaptation for desiccation, a stress they likely experience frequently and can survive, has given them an ability to recognize and respond to DNA damage and hence a cross-tolerance to IR[11,19]. Long-term desiccation can also result in genome instability and DNA damage[43,44]. Although we did not see a wide-scale correlation between the transcriptomic responses to desiccation and irradiation (Figure 3), we revisited these data to specifically investigate if DNA repair transcripts were enriched in response to desiccation[30,31]. We did see a slight enrichment in some transcripts of the BER and TMEJ pathways in *H. exemplaris* (Figure S5), but this enrichment was below Log_2FC of 2, not nearly as strong as the enrichment observed after IR exposure. While both dried animals and animals entering desiccation did not show strong enrichment of DNA repair transcripts, it remains possible that these transcripts could be robustly expressed later, upon rehydration. It remains enigmatic why tardigrades have evolved strong IR tolerance. Additionally, there are many tardigrade species that are adapted to marine and freshwater environments and do not tolerate desiccation[58]. Expanding the study of IR tolerance to these desiccation-intolerant species will help us to gain a better understanding of the relationship between IR tolerance and desiccation tolerance mechanisms.

Transcriptional responses to IR have been interrogated in other organisms including bacteria, *Drosophila melanogaster,* and human cell lines. While bacteria can upregulate DNA repair genes in response to DNA damage[59], enrichment of some of these transcripts in *Drosophila* and humans has been found to be at a typically modest level of only 1.5-3 fold (dose of IR ranging from 2-864 Gy for *Drosophila* and 3-10 Gy for humans, source either X-ray or Cs^{137}) [24–29]. The level to which *H. exemplaris* enriches these DNA repair transcripts, and the number of repair gene transcripts enriched, are by comparison far more extreme, and likely makes an important contribution to the extreme IR tolerance of some tardigrade species. We also found two histone subunits highly upregulated upon IR exposure (Table S1). Since we used poly(A) selection to isolate mRNA, these are likely to be poly(A)-containing mRNAs and hence non-cell cycle regulated histones that are typically used outside of S phase DNA replication cycles[60]. We

speculate that these strongly upregulated histones might contribute to forming new nucleosomes after DNA repair in *H. exemplaris*. Additionally, we identified that the DNA repair transcripts we investigated via *in situ* hybridization enrich in many tissues, and with stronger enrichment in certain tissues. The tissue specificity of enrichment did not suggest to us that different tissues use different upregulated DNA repair pathways (as an example, enrichment in ovary was seen for both *PCNA* (BER) and *XRCC5* (NHEJ)). It is currently unclear why these transcripts are enriched in a tissue-specific manner and if it is important to the ability of *H. exemplaris* to survive high levels of IR. A potential explanation for enrichment of these transcripts in stylet glands, claw glands, and hindgut could be that each of these tissues is involved in cuticle formation and responsible for replacing the cuticle of their respective structures upon molting[49]. Our protocol for irradiation and staining included the use of freshly molted adults (within 24 hours of molting) which may have selected for a time when these tissues would be relatively transcriptionally active during the molting process. Transcriptionally active regions are more susceptible to DNA damage from IR[61], so potentially these tissues experience more DNA damage and upregulate the transcription of these genes disproportionately in response. However, we did not see evidence from our TUNEL experiments that these tissues experienced more damage than others throughout the body.

Prior to this study, the only established mechanism of tardigrade IR tolerance was a protective mechanism that prevents damage, conferred by the *R.* cf. *varieornatus* Dsup protein[15–17]. Despite *H. exemplaris* having a Dsup protein[16], the transcription of their Dsup gene does not significantly respond to IR (Log_2FC of -0.57 after 500 Gy, Data S1B), and we found evidence for a response involving DNA repair genes rather than exclusively DNA protection. It is possible that the *H. exemplaris* Dsup does not have the same protective function as the *R.* cf. *varieornatus* Dsup due to sequence divergence[16]. We expressed both version of the *Dsup* gene in *E. coli*, and in this heterologous condition only the *R.* cf. *varieornatus* Dsup protein conferred IR tolerance to bacteria (Figure 5B). Dsup is limited to a few eutardigrade lineages, and even within those lineages it is unclear to what extent Dsup plays a role in IR tolerance *in vivo*[16,18–20]. Even though *R.* cf. *varieornatus* Dsup was shown to protect DNA from IR damage in HEK 293T cells, overexpression of this same protein in human neuronal cells resulted in increased DNA damage[15,16,62]. These discrepancies in Dsup distribution and action suggest that different tardigrade lineages have likely evolved different mechanisms for dealing with IR-related DNA damage. In support of this idea is evidence for the lack of canonical NHEJ repair in heterotardigrades[18]. Our results suggest that *H. exemplaris* may survive IR at least in part through NHEJ-mediated DNA repair. However, the heterotardigrade *E.* cf. *sigismundi* entirely

lacks canonical NHEJ components[18]. Intriguingly this species, although radiation tolerant, has a lower LD50 than *H. exemplaris* (1600 Gy vs 4000 Gy)[19]. The lack of NHEJ mechanisms in *E.* cf. *sigismundi* suggests that heterotardigrades may rely on different mechanisms for dealing with IR-related DNA damage. Recently, ongoing work identified an additional tardigrade unique protein with DNA protective abilities[42]. This protein (Tardigrade DNA damage Response protein, TDR1) is more widely conserved across tardigrade phylogeny compared to Dsup and possesses the ability to reduce DNA damage in human U2OS cells exposed to bleomycin[42], suggesting that TDR1 is another mechanism that some tardigrades may employ to combat IR stress. The results of previous work[15–19,42,63] in combination with the results of this study suggest the possibility of synergy between protective and repair mechanisms in tardigrade IR tolerance. If some tardigrades use both mechanisms, the protective mechanism could work at IR levels at which DNA damage could be prevented or slow the accumulation of damage at higher IR levels, and as damage accumulates this could activate the transcription of DNA repair pathway genes that remedy the damage. Understanding how different mechanisms of IR tolerance might work together, as well as uncovering additional tolerance mechanisms from a wider range of tardigrade species, are intriguing avenues for future research.

ACKNOWLEDGMENTS: We thank Nipam Patel and Jenny McCarthy for assistance with the adaptation of TUNEL protocols for tardigrades, the UNC High Throughput Sequencing Facility and the UNC Biology Microscopy Core for technical assistance, Dale Ramsden, Aziz Sancar, Greg Matera, Tom Petes, Corbin Jones, Hemant Kelkar, Dan Janies, and members of the Ramsden and Goldstein labs for helpful feedback and discussions, and Adriana Schlachter for assistance with the CellProfiler analysis. This work was supported by NSF grant IOS 2028860 to BG and MCB 2149172 to LMH. JDH was supported by the NIH (F32GM131577) and ERS was supported by the NSF Graduate Research Fellowship progam. The Q Exactive HF-X mass spectrometer was funded via an NSF Major Research Instrumentation award (CHE-1726291).

AUTHOR CONTRIBUTIONS: Conceptualization, CMCH, BG; Methodology, CMCH, JDH, TD, ERS; Formal Analysis, CMCH; Investigation, CMCH, JDH, TD, ERS; Writing - Original Draft, CMCH; Writing - Reviewing and Editing, CMCH, JDH, TD, ERS, LMH, BG; Visualization, CMCH; Supervision, BG; Funding Acquisition, BG, JDH, ERS, LMH.

DECLARATION OF INTERESTS: The authors declare no competing interests.

MAIN TEXT FIGURE LEGENDS

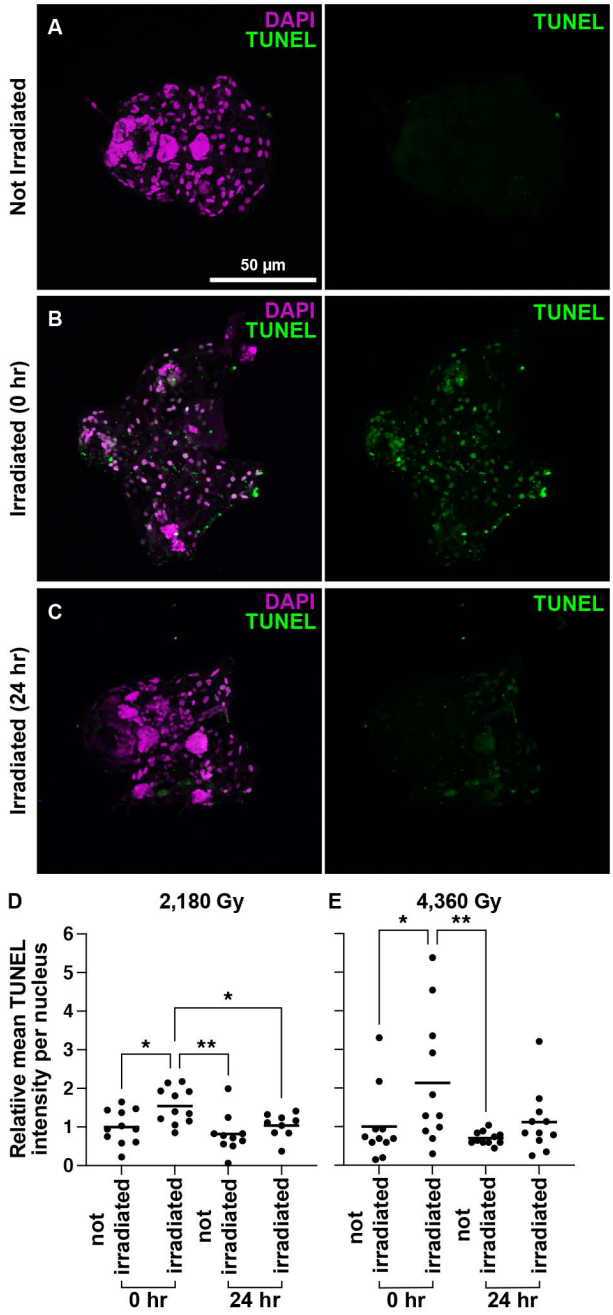

Figure 1. Visualizing DNA damage in tardigrades following ionizing radiation exposure. (**A-C**) Representative images of TUNEL signal in individuals that were not exposed to IR (**A**), exposed to 4,360 Gy IR (**B**), and exposed to 4,360 Gy IR and allowed to recover for 24 hours (C). The TUNEL signal shown here generally covers entire nuclei and is not obviously localized to subnuclear structures. Animals were physically disrupted for TUNEL protocol so above images are fragments of whole adults. Orientation and region of animal in image are as follows: (**A**) dorsal up, includes head and first and second leg-bearing segments, (**B**) ventral up, includes

second and third leg-bearing segments, (**C**) ventral up, includes head and first and second leg-bearing segments. Anterior is to the left. Scale bar applies to all images. (**D and E**) Plots displaying the relative mean intensity of TUNEL signal per nucleus for 2,180 Gy (**D**) and 4,360 Gy (**E**) IR exposure. For each plot the groups from left to right are as follows: not exposed to IR, exposed to IR, not exposed to IR and left for 24 hours, exposed to IR and allowed to recover for 24 hours, (n=11 individuals for all groups, except 2,180 Gy not irradiated 24 hr (n=10) and 2,180 Gy irradiated 24 hr (n=9)). A one-way ANOVA followed by a post-hoc Dunnett test to the mean of the irradiated timepoint 0 for each experiment was used to determine significant differences between treatment groups. Significance is as follows: *p<.05 ** p<.01. 2,180 Gy 0 hr vs. not irradiated 0 hr: p=.02, vs. not irradiated 24 hr: p=.002, and vs irradiated 24 hr: p=.04. 4,360 Gy 0 hr vs not irradiated 0 hr: p=.04, vs not irradiated 24 hr: p=.008, and vs irradiated 24 hr: p=.07. See also Data S1A.

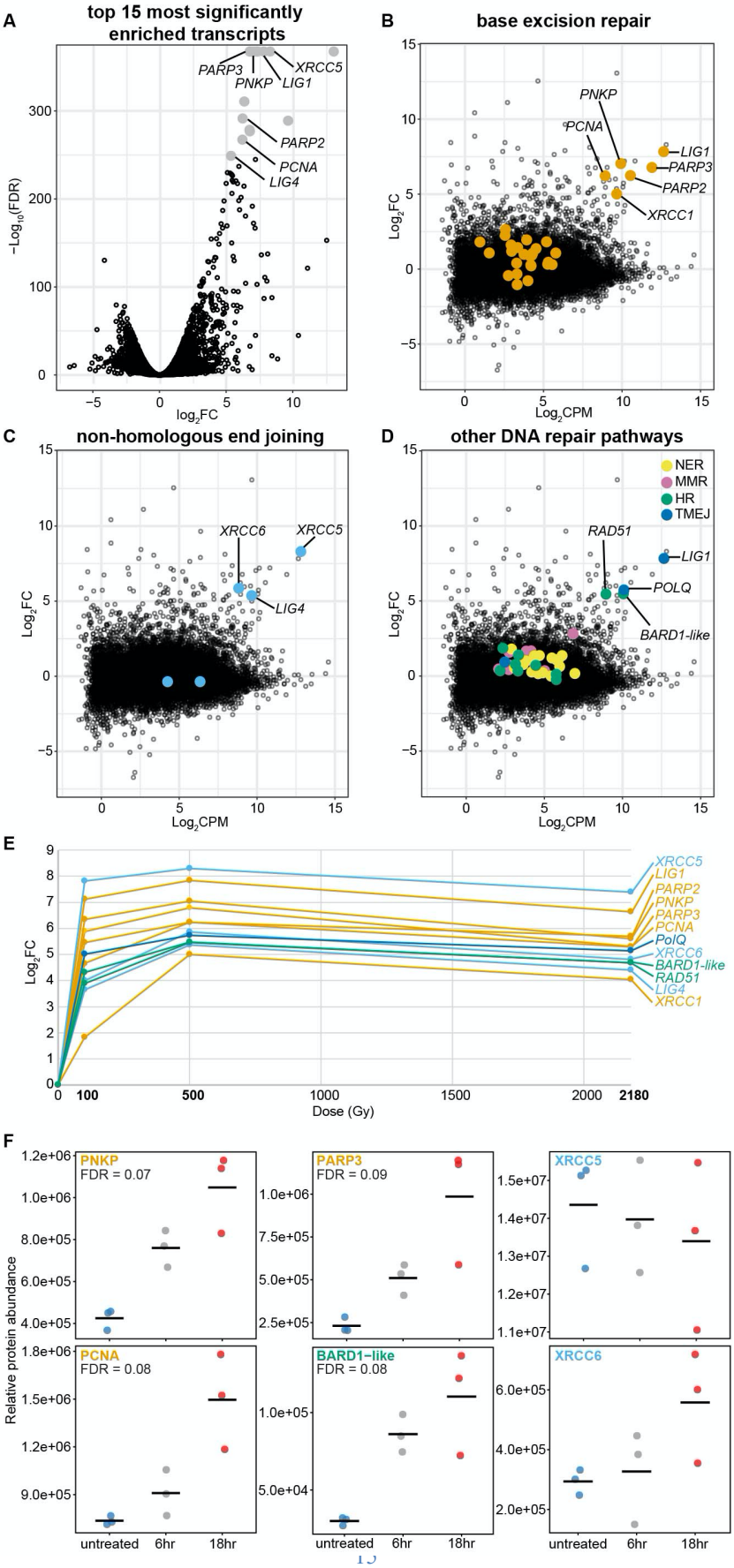
A
top 15 most significantly enriched transcripts
PARP3
PNKP
LIG1
XRCC5
PARP2
PCNA
LIG4
−Log10(FDR)
log2FC
B
base excision repair
PNKP
PCNA
LIG1
PARP3
PARP2
XRCC1
Log2FC
Log2CPM
C
non-homologous end joining
XRCC6
XRCC5
LIG4
Log2FC
Log2CPM
D
other DNA repair pathways
NER
MMR
HR
TMEJ
RAD51
LIG1
POLQ
BARD1-like
Log2FC
Log2CPM
E
XRCC5
LIG1
PARP2
PNKP
PARP3
PCNA
PolQ
XRCC6
BARD1-like
RAD51
LIG4
XRCC1
Log2FC
Dose (Gy)
F
PNKP
FDR = 0.07
PARP3
FDR = 0.09
XRCC5
PCNA
FDR = 0.08
BARD1−like
FDR = 0.08
XRCC6
Relative protein abundance
untreated
6hr
18hr

Figure 2. *H. exemplaris* increases expression of certain DNA repair transcripts and proteins in response to ionizing radiation. (**A**) Volcano plot of Log_2FC by $-Log_{10}(FDR)$ showing the transcriptional response of *H. exemplaris* to 500 Gy IR. The top 15 most significantly enriched transcripts (by FDR) are marked in gray. DNA repair pathway genes among the top 15 are labeled. (**B-D**) MA plots displaying Log_2FC of *H. exemplaris* transcripts in response to 500 Gy IR with (**B**) transcripts encoding BER proteins marked in orange, (**C**) transcripts encoding NHEJ proteins marked in light blue, and (**D**) transcripts encoding NER, MMR, HR, and TMEJ proteins marked in yellow, pink, green, and dark blue, respectively. Transcripts encoding DNA repair proteins that are significantly enriched are indicated by name. Note that LIG1 functions in two pathways. (**E**) Plot showing Log_2FC for selected enriched DNA repair transcripts at 100, 500, and 2180 Gy doses of IR. Colors are the same as in MA plots. LIG1 is colored as BER (orange), but also functions in TMEJ (dark blue). **(F)** Relative protein abundance for DNA repair proteins 6 and 18 hours after exposure to 500 Gy IR. See also Table S1-S4, Figure S6, and Data S1B.

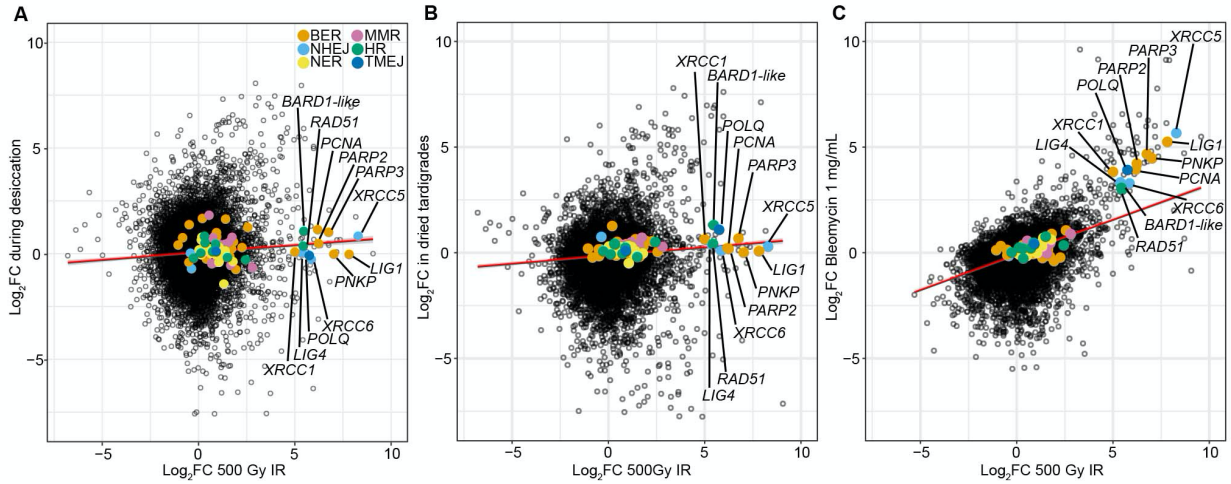

Figure 3: *H. exemplaris* transcriptomic responses to desiccation and ionizing radiation do not correlate, but transcriptomic responses to ionizing radiation and bleomycin do. (**A-C**) Plots showing the Log_2FC of transcripts during desiccation (**A**) in dried tardigrades (**B**) and after a 24 hour treatment with 1 mg/mL bleomycin (**C**) plotted against the Log_2FC of transcripts in response to 500 Gy IR. Original data for the transcriptional response to desiccation are from [30,31] (**A**) and [32] (**B**). Pearson correlation test, r^2 for the trendlines is 0.003468, 0.003224, and 0.2103, respectively. Colors are the same as in Figure 2. LIG1 is colored as BER (orange), but also functions in TMEJ (dark blue). See also Figure S1 and S6, Table S1-S4, and Data S1C.

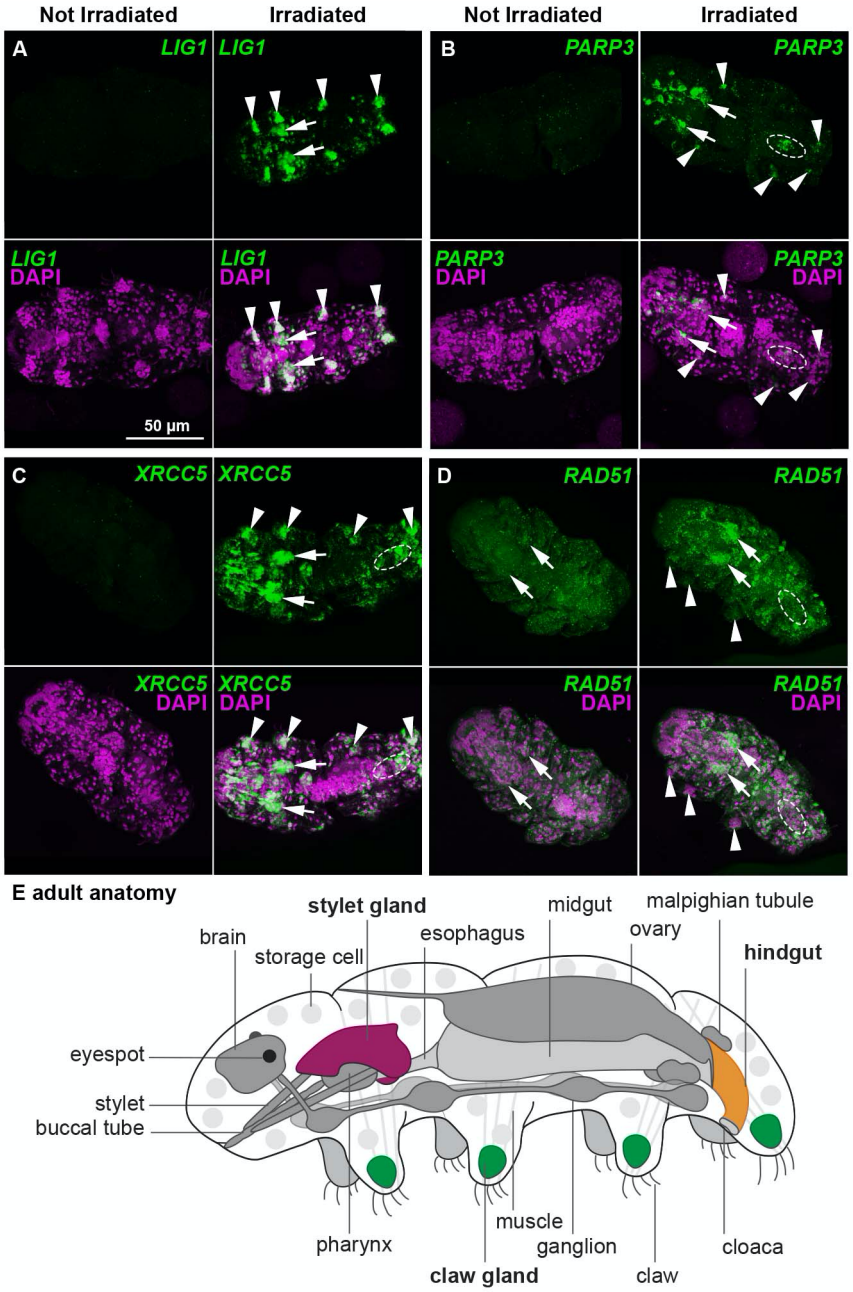

Figure 4. Tissue-specific enrichment of DNA repair transcripts in *H. exemplaris* following ionizing radiation exposure. (**A-D**) Representative images of *in situ* hybridization for DNA repair transcripts with and without exposure to 100 Gy ionizing radiation. Exposure and contrast were adjusted to visualize regions of most intense signal. Expression in stylet glands (arrows), claw glands (arrowheads), and hindgut (dashed outlines) is indicated where seen. Transcripts encoding members of the (**A**) TMEJ, (**A-B**) BER, (**C**) NHEJ, and (**D**) HR pathways are represented. Scale bar in A applies to all images. Anterior is to the left. Orientation of each image is as follows: (**A**) ventral up (**B-C**) dorsal up. (**E**) Schematic of a lateral view of an adult tardigrade with stylet glands (burgundy), claw glands (green), hindgut (orange), and other

landmark structures (gray) indicated (adapted from [64]). Some anatomical features are not shown in this diagram. See also Figure S2-S4.

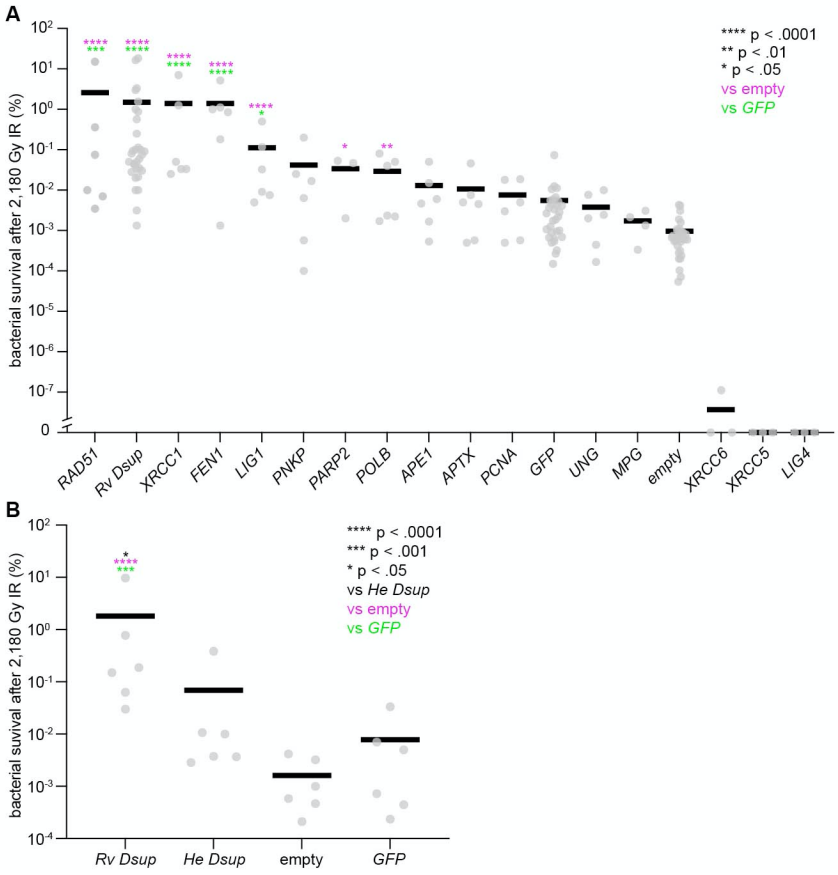

Figure 5. High levels of certain DNA repair genes are sufficient to improve bacterial survival after ionizing radiation exposure. (**A**) Plot of tardigrade DNA repair transcripts organized from most efficient (left) to least efficient (right) at improving bacterial IR survival, including controls (GFP and empty). N=6 for all transcripts except for *Rv Dsup* (N=31), *PARP2* (N=3), *MPG* (N=4), GFP (N=31), empty (N=31), *XRCC6* (N=3), *XRCC5* (N=3), and *LIG4* (N=3). Significance is only indicated for those transcripts that show significantly improved survival relative to bacteria carrying the *GFP* expressing vector or empty vector. (**B**) Expression of *R.* cf. *varieornatus Dsup* but not *H. exemplaris Dsup* in bacteria improved bacterial survival after exposure to ionizing radiation compared to controls (GFP and empty). N=6 for all transcripts. See also Figure S5 and Data S1D.

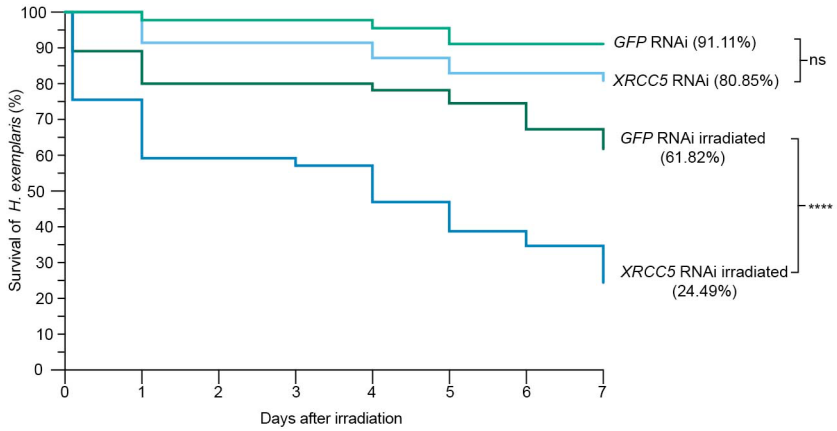

Figure 6. High levels of XRCC5 are important for tardigrade ionizing radiation survival. Survival curves tracking the percent survival of animals following RNAi through 7 days after exposure to 2,180 Gy IR. Groups are as follows: *GFP* RNAi Control (light green, n=45), *XRCC5* RNAi Control (light blue, n=47), *GFP* RNAi irradiated (dark green, n=55), and *XRCC5* RNAi irradiated (dark blue, n=49). **** = p<.0001 (log-rank test). See also Data S1E.

STAR METHODS

RESOURCE AVAILABILITY

Lead contact

Further information and requests for resources and reagents should be directed to and will be fulfilled by the lead contact, Courtney Clark-Hachtel (clarkcm6@email.unc.edu)

Materials availability

Plasmids used for bacterial expression experiments are available upon request.

Data and code availability

- All data are available in the manuscript or the supplementary materials. RNA sequencing data is available through NCBI Gene Expression Omnibus (accession: GSE253471). The mass spectrometry proteomics data have been deposited to the ProteomeXchange Consortium via the PRIDE[65] partner repository with the dataset identifier PXD047724 and 10.6019/PXD047724.
- This paper does not report original code.
- Any additional information required to reanalyze the data reported in this paper is available from the lead contact upon request.

EXPERIMENTAL MODEL AND STUDY PARTICIPANT DETAILS

Tardigrade culture

Cultures of parthenogenetic *H. exemplaris* (Z151) were maintained as previously described[66,67]. Animals were reared in 35 mm vented petri dishes (Tritech Research, T3500) with approximately 2 mL of Deer Park brand spring water and 0.5 mL Chloroccocum sp. algae (Carolina Biological Supply). Freshly molted adult females were used for all experiments.

METHOD DETAILS

Tardigrade irradiation

Gravid animals were collected and allowed to lay embryos and molt overnight. Freshly molted animals were placed into a 1.5 mL microcentrifuge tube in 100 µL of clean spring water (deer park) and then placed into a Gammator B Cs^{137} source gamma irradiator (current dose rate

1.4251 Gy/minute). Animals were left in the irradiator for an appropriate amount of time to reach the desired dose for each experiment (see below).

Terminal deoxynucleotidyl transferase dUTP nick end labeling (TUNEL) assays, imaging, and analysis

Treated animals were irradiated as described above to a dose of either 2,180 Gy (24 hours) or 4,360 Gy (48 hours). Control animals were prepared in the same way as treated animals and remained on the lab bench for the same amount of time as their treated counterparts. Upon completion of irradiation, animals were either fixed immediately for TUNEL analysis or allowed to recover for 24 hours on the laboratory bench and then fixed. At least 20 animals were prepared for each treatment (not irradiated and irradiated 0 hr, and not irradiated and irradiated 24 hr). Fixation was performed in 4% paraformaldehyde (PFA) in Phosphate-Buffered Saline (PBS) with 0.1% TritonX (0.1% PBT) overnight at 4°C. The fixative was washed out with 0.1% PBT. Animals were permeabilized by manual cutting with a syringe needle followed by sonication with a Branson Sonifier 250 probe sonicator (1 pulse, output control: 4, duty cycle: 50). The tardigrades were then transferred to a Mobicol column with 10 µm pore filter (Boca Scientific, M2210) in 0.1% PBT. Animals were subjected to a gradual methanol dehydration series from 25% to 100% methanol:0.1%PBT and left in -20°C to dehydrate overnight. Animals were gradually rehydrated from 100% to 0% methanol:0.1% PBT. The TUNEL assay protocol for tardigrades was adapted from a protocol for brine shrimp (McCarthy and Patel, personal communication) and for *Drosophila melanogaster* [68]. Briefly, tardigrades were further permeabilized by incubating in Proteinase K (10 µg/mL) for 5 min at room temperature (RT) followed by incubations in *in situ* detergent (30 minutes, RT, shaking), 0.3% PBT Sodium deoxycholate (30 minutes, RT, shaking), and sodium citrate (1 hour, 65ºC, shaking). TUNEL staining was performed as in [68] using the TMR red *in situ* cell death detection kit (Roche, 12156792910).

Stained animals were mounted in DAPI fluoromount-G (Southern Biotech) with 28.41 µm mounting beads (whitehouse scientific). Animals were imaged on a Zeiss 880 LSM with fast Airyscan detector. At least 9 individuals were imaged from each treatment for downstream analysis. 3D z-stacks were processed with FIJI [69] and saved as separated channel .tif files for processing in CellProfiler[70]. Nuclei were segmented following the 3D segmentation of cell monolayer tutorial (tutorials.cellprofiler.org) through the “resize objects” as nuclei step. The mean intensity of TUNEL signal per nucleus was calculated in CellProfiler using the “measure object intensity” module on identified nuclei in CellProfiler[70]. Nuclear TUNEL intensity

measurements were exported and the average “mean intensity” value was used for downstream analysis. Nuclear TUNEL intensity values were normalized to the mean of the not irradiated 0 hr samples for each experiment.

Tardigrade bleomycin treatment and survival analysis

Bleomycin sulphate powder (Sigma BP971) was resuspended to a concentration of 100 mg/mL in spring water and then serially diluted in spring water to make additional working solutions of 10 mg/mL, 1 mg/mL, 100 µg/mL, and 10 µg/mL. Gravid animals were collected and allowed to lay embryos and molt overnight. Freshly molted animals were placed into a 1.5 mL microcentrifuge tube in spring water. The spring water was removed and replaced with bleomycin solution in spring water at the desired concentration. Animals were soaked in the bleomycin solution or plain spring water (controls) for 24 hours in sealed microcentrifuge tubes. Three trials of 10-20 animals each were performed for each dose of bleomycin (and control). After treatment, animals were rinsed with clean spring water five times before being moved to 96-well plates with one animal/well filled with 100 µL spring water (Deer Park brand) and ~5 µL of *Chloroccocum* algae (Carolina Biological Supply). Survival and egg laying was checked approximately daily and the individuals in each well of the 96-well plate were scored as alive (movement detected) or dead (movement not detected) over the course of 7 days to monitor survival. On day 7 adults were removed from the wells, and wells were monitored for an additional 6 days for egg hatching (normal developmental time for *H. exemplaris* is 4.5 days[67]). Laying is reported as the percent of observed animals that laid clutches and hatching is reported as the percent of observed laying animals that had viable clutches (Figure S1).

RNA sequencing

Approximately 200 adult animals were used for each replicate (IR experiment: 3 replicates each of unirradiated, 100 Gy, 500 Gy, and 2,180 Gy; bleomycin experiment: 3 replicates each of 1 mg/mL, 100 µg/mL, 10 µg/mL). For IR, animals were exposed to an appropriate dose of IR (or left on the lab bench for 24 hours, unirradiated). For bleomycin experiments, animals were soaked in the desired concentration of bleomycin:spring water or spring water (controls) for 24 hours. For both experiments, RNA was isolated immediately from each replicate using the PicoPure RNA isolation kit (Applied Biosystems) following slightly modified manufacturer instructions. Libraries were constructed using the KAPA mRNA stranded library prep kit and fragmented to ~300bp. Paired end sequencing (2 x 50bp) was performed using the Illumina NextSeq2000 platform. Reads were adapter trimmed then mapped to the most recent genome

for *H. exemplaris* (v3.1.5) using BBduk and BBmap (ver 39.01), and counts were assigned with featureCounts[71] (ver 2.0.6) using the annotation file associated with this genome. Reads were aggregated at the level of genes and only genes with more than one count in at least two samples were kept for differential expression analysis. Transcript abundance, fold changes, and FDR values were determined using EdgeR (Data S1B and S1C)[72]. For GO term analysis, Trinotate[73] ver 4.0.2 was used with default parameters, with terms parsed from the Pfam results column using a custom Python script.

Protein extraction and mass spectrometry analysis

Approximately 10,000 tardigrades were collected per sample (3 replicates each of untreated, irradiated with 500 Gy and left to recover for 6hr, and irradiated with 500 Gy and left to recover for 18hr). Following recovery, animals were ultrasonicated in 500 µL 20 mM HEPES using a Covaris E220 Focused-ultrasonicator for four 1-minute rounds at 150 W, 15% duty cycle, and 250 cycles/burst at 4°C. Samples were clarified, and proteins were precipitated using 100 mM ammonium acetate in methanol. Pellets were resuspended in 4 M urea in 100 mM Tris-HCl pH 7.2. For each sample, 30 µg of protein were reduced with 10 mM dithiothreitol (DTT), alkylated with 30 mM iodoacetamide (IAM), and precipitated using 100 mM ammonium acetate in methanol. Proteins were resuspended in 2 M urea in 100 mM Tris-HCl pH 7.2 and digested overnight (>16hr) using 1 µg of Trypsin Gold (Promega) at 37°C. High pH reversed-phase offline fractionation was performed using 20 mM ammonium formate pH 10 in water as mobile phase A and 100% acetonitrile as mobile phase B. Samples (400 µL) were injected onto an XBridge™ Peptide BEH C18 column (300 Å, 2.5 µm, 3.0 x 100 mm; Waters) and were separated over a 75 min linear gradient using a 300 µL/min flow rate. Fractions were collected starting at 10 min in 6-min intervals up until 46 min, yielding 6 total fractions. For each sample, the first and second fractions and fifth and sixth fractions were combined, giving four total fractions per sample. Fractions were then desalted using C18 ZipTips (Millipore Sigma). Fractions were analyzed using a nanoAcquity UPLC (Waters) coupled to a Q Exactive HF-X (Thermo Fisher Scientific). Mobile phase A consisted of 0.1% FA in water, and mobile phase B consisted of 0.1% FA in acetonitrile. Fractions were injected (4 µL) onto a Symmetry C18 Trap Column (100 Å, 5 µm, 180 µm x 20 mm; Waters). Trapping occurred for 3min at a 5 µL/min flow rate at 99% mobile phase A and 1% mobile phase B. Peptides were then separated using a HSS T3 C18 column (1.8 µm, 75 µm x 250 mm; Waters) using a 2 hr method at 300 nL/min. Mass spectrometry analysis occurred in a data dependent manner, with survey scans collected over a 350-2000 *m/z* range at 120,000 resolving power. Fragmentation scans for the top 20 ions

within a survey scan were acquired with a normalized collision energy set at 28 over a 200-2000 m/z range at 30,000 resolving power.

Proteomics database searching and protein quantification

Raw files from the same fractions across replicates and conditions were imported into Progenesis QI for Proteomics (Nonlinear Dynamics, version 4.2) for peak picking and alignment. For example, Fraction 1 from the Untreated, Irradiated 6hr recovery, and Irradiated 18hr recovery across all biological replicates were processed together. A combined peak list (.mgf) containing all fragmentation spectra for each feature *m/z* was exported for peptide sequence identification using Mascot (Matrix Science, version 2.5.1). Database searching was performed against the *H. exemplaris* UniProt proteome (https://www.uniprot.org/uniprotkb?query=(taxonomy_id:2072580) and sequences for common laboratory contaminants (https://www.thegpm.org/crap/,116 sequences). MS/MS data were searched using precursor/product ion tolerances of 15 ppm/0.02 Da, trypsin specificity with two possible mixed cleavages, fixed cysteine carbamidomethylation, and variable modifications of methionine oxidation and N-terminus acetylation. Identified peptides were analyzed in custom scripts written in R (https://github.com/hickslab/QuantifyR). For peptides that were identified in multiple fractions from the same replicate, the abundances were summed to give a total peptide abundance for that sample. Due to the possibility of missing values from offline fractionation affecting protein-level quantification within the experiment, peptides that had a coefficient of variation >0.40 in all conditions were removed from subsequent analysis. Protein quantification was achieved using a Hi-3 method[74]. Peptide abundances across all conditions were averaged. The three peptides with the highest averages for each protein were then used for protein quantification. Using the most abundant peptides across conditions as described, the three peptide abundances were averaged for the individual replicates to obtain a representative protein abundance for each protein detected in each sample. Proteins that did not have at least 2 unique peptides identified were removed from further analysis. Proteins that did not have one condition with >50% nonzero values from the determined protein abundance were also removed from further analysis.

Gene homolog identification and cloning

Homologs of canonical DNA repair proteins of *H. exemplaris* were identified in a previous study [18] and updated to the current genome annotation (v3.1.5) using BLAST P. The homology of these proteins to their presumed DNA repair proteins was also confirmed by reciprocal BLAST

to human and *Drosophila melanogaster* protein databases. A putative *H. exemplaris* Dsup protein was previously identified in[16]. *H. exemplaris* POLQ was identified via BLAST P using human POLQ protein (NP_955452.3) as a query and confirmed via reciprocal BLAST. BARD1-like and BARD1-like C-terminal domain were identified via reciprocal BLAST. The partial Ku70 protein that is enriched upon exposure to IR (BV898_07145) was identified via an NCBI Domain search on the putative protein. This protein is predicted to only contain the N-terminal portion of Ku70 and lacks the domains responsible for interaction with Ku80 and DNA[34]. Based on homolog transcript sequence, primers were designed to clone the full-length transcript from tardigrade cDNA or from GBlock synthesized gene fragments (IDT: *Rv Dsup, He Dsup, and RAD51*). Primers were designed with a 30bp overlap with the pDest17 expression vector (Invitrogen: 11803012) for subsequent incorporation into this vector via Gibson assembly.

in situ hybridization and expression scoring

Templates for *in situ* hybridization probes were amplified from vectors containing the full-length gene using the primers listed in Table S5. Antisense RNA probes for *in situ* were synthesized as previously described[75,76], purified using an RNA clean and concentrator kit (Zymo, R1015), and eluted in RNAse free water. The final concentration of probes for *in situ* reactions was 0.5 µg/mL as previously recommended[76].

Tardigrades for *in situ* expression analysis were exposed to a dose of 100 Gy IR and fixed immediately for *in situ* hybridization in 4% PFA in PBS with 0.1% Tween20 (0.1% PTW) overnight at 4°C [77]. Controls were left on the lab bench for the equivalent amount of time. Fluorescent *in situ* hybridization was performed in adults as previously described[77]. At least two replicates with 10 animals each were performed for each DNA repair transcript analyzed for both irradiated and control experiments. Animals were mounted with DAPI fluoromount-G (Southern Biotech) with 28.41 µm mounting beads (whitehouse scientific) and imaged on a Zeiss 880 LSM with fast Airyscan detector.

in situ hybridization expression profiles were examined in detail for at least 3 control and 3 treated individuals for each DNA repair transcript that we examined. Individuals were imaged at both lower laser power (appropriate setting for tissues with high expression) and higher laser power (to facilitate the observation of expression in tissues with lower levels of expression). Tissues were identified based on morphological analysis and informed by[48]. Expression in each structure was scored from the higher laser power images on a scale from 0 (no observed expression) to 3 (observed oversaturated expression). A score of 1 indicates minimally observed expression and 2 indicates slightly undersaturated observed expression. Each tissue

was scored within an individual and then a mean expression score for each tissue was calculated by averaging the tissue scores across individuals (Figure S4).

Bacterial protein expression and irradiation

pDest17 vectors containing full-length versions of individual tardigrade DNA repair transcripts were expressed in *E. coli* BL21 AI cells (Invitrogen, C607003) to determine if heterologous expression could confer tolerance to IR. The sequence of the expression vectors was confirmed before transformation into BL21 AI cells. Bacteria were grown overnight in 5 mL LB with Ampicillin and diluted 1:20 into LB with Ampicillin and 0.2% L-arabinose to induce expression from the pDest17 vector. Cultures were induced for 4 hours at 37°C while shaking. After 4 hours the OD600 of the cultures was measured. Induced cultures of bacteria expressing each DNA repair transcript were split into two 1.5 mL microcentrifuge tubes and densities were normalized by dilution into 1 mL total culture. Treated bacteria were exposed to a dose of 2,180 Gy IR while their control counterparts remained on the laboratory bench, both under continual induction. After treatment, A dilution series of both treated and untreated bacteria was plated to determine the number of colony forming units (cfu). Percent survival was calculated as the cfu after irradiation divided by the cfu for untreated cells expressing the same DNA repair component.

Analysis of heterologous protein expression in bacteria

Expression of protein in bacteria was analyzed by SDS-PAGE. Following the same induction protocol as used for irradiation experiments (see above), bacteria were pelleted by centrifugation, resuspended in 200 µL 0.85% NaCl, and lysed with a Branson Sonifier 250 probe sonicator (30 pulses, output control: 5, duty cycle: 50%). The soluble fraction of lysate was isolated by centrifuging at 14,000 rpm for 10 minutes at 4°C and retaining only the supernatant. Protein concentrations were quantified with Bio-Rad protein assay (Bio-Rad, 5000006).

Protein (2 µg total lysate, 5 µg soluble lysate) was loaded onto 4-12% Bis-Tris NuPAGE minigels (Invitrogen, NP0322BOX). 10 µL of precision plus protein kaleidoscope prestained standard (Bio-Rad, Cat#1610375) was included as a standard on each gel. Gels were run in 1x NuPAGE MOPS SDS running buffer (Invitrogen, NP0001) at 140 V for 75 minutes. Gels were stained in Coomassie and destained in a solution of 5:4:1 water:methanol:acetic acid before imaging (Figure S5). The expected molecular weights of proteins that are reported were computed with the Expasy Compute pI/Mw tool [78].

dsRNA synthesis and injection

DNA templates for synthesis of double-stranded RNA (dsRNA) for *XRCC5* and *GFP* were amplified using the primers indicated in Table S5. dsRNA for both *XRCC5* and *GFP* were synthesized as previously described[30], purified by isopropanol precipitation, and eluted in RNAse free water. dsRNA was diluted to a concentration of 1µg/uL in RNAse free water for injection. Gravid females for injection were isolated and allowed to lay eggs and molt overnight prior to injection. Adult tardigrades were injected with dsRNA targeting either *XRCC5* or *GFP* as previously described[53,79].

RNAi Survival assays

Following injection with dsRNA targeting either *XRCC5* or *GFP* animals were allowed to recover overnight. After recovery, animals injected with either dsRNA were divided into two groups and placed into 1.5 mL microcentrifuge tubes. One group was exposed to 2,180 Gy IR and the other was left on the laboratory bench for an equivalent amount of time (24 hours). After treatment, animals were collected and placed into a 96-well plate with one animal/well filled with 100 µL spring water (Deer Park brand) and ~5 µL of *Chloroccocum* algae (Carolina Biological Supply). IR exposure did cause some lethality on day 0 (the day animals were removed from the irradiator) in some groups (Figure 6). These animals were still transferred to 96-well plates along with surviving animals. Survival was checked approximately daily and the individuals in each well of the 96-well plate were scored as alive (movement detected) or dead (movement not detected) over the course of 7 days.

QUANTIFICATION AND STATISTICAL ANALYSIS

For the TUNEL experiments a one-way ANOVA followed by a post-hoc Dunnett test to the mean of the irradiated timepoint 0 for each experiment was used to determine significant differences between treatment groups (Prism). All statistical analyses for mRNAseq were performed using EdgeR (Transcript abundance, fold changes, p- and FDR values)(Data S1B and S1C)[72]. Pearson correlation tests were run in R[80] to evaluate the correlation between mRNAseq libraries from different stresses. For differential global proteomic analysis, statistical analysis was performed using a two-sided student's t-test with a Benjamini and Hochberg (BH) method used for p-value correction[81]. Fold change was calculated by the difference of mean abundance values for each protein across conditions. Only observations with an FDR <0.05 and a $Log_2FC \geq 1$ were considered statistically significantly different. In the bacterial expression experiments, the percent survival was log transformed to standardize variance for statistical

analysis as previously described[82]. A one-way ANOVA followed by a post-hoc Dunnett test to the means of the control groups (empty and GFP) was then used to determine significant improvement in survival relative to controls following IR exposure (Prism). The survival data for RNAi assays was converted to survival curves in Prism and subjected to Kaplan-Meier simple survival analysis to determine significant differences in survival between groups (Figure 6). All statistical details for reported experiments can be found in the associated Figure and Figure legend.

SUPPLEMENTAL ITEMS

Data S1: Detailed data underlying main and supplemental Figures. Related to Figures 1, 2, 3, 5, 6, S1, S4, and S6. (**A**) Raw TUNEL mean intensity data underlying Figure 1D and E. (**B**) EdgeR output for 500 Gy, 100 Gy, and 2,180 Gy IR treatments. Also includes GO and protein enrichment analysis for 500 Gy IR. (**C**) EdgeR outputs merged by Gene ID for during desiccation vs. 500 Gy IR, dried vs. 500 Gy IR, and 1 mg/mL bleomycin vs. 500 Gy IR. (**D**) Raw percent survival data for *E. coli* expressing different tardigrade DNA repair/protection genes or control genes. (**E**) Raw percent survival data for *H. exemplaris* after RNAi for *XRCC5* or *GFP* and radiation treatment. (**F**) Raw survival, laying, and hatching data following treatments with varying concentrations of bleomycin. Also includes the EdgeR output for 10 and 100 µg/mL bleomycin treatments. (**G**) *in situ* expression scoring data by tissue for each gene. (**H**) EdgeR output for DNA repair genes during desiccation and in dried tardigrades.

Figures S1-S6

Tables S1-S5

REFERENCES

1. Boothby, T.C. (2019). Mechanisms and evolution of resistance to environmental extremes in animals. Evodevo *10*, 30. 10.1186/s13227-019-0143-4.

2. Teets, N.M., Gantz, J.D., and Kawarasaki, Y. (2020). Rapid cold hardening : ecological relevance , physiological mechanisms and new perspectives. J. Exp. Biol. *223*, jeb203448. 10.1242/jeb.203448.

3. Schulte, P.M. (2014). What is environmental stress? Insights from fish living in a variable environment. J. Exp. Biol. *217*, 23–34. 10.1242/jeb.089722.

4. Shaikhutdinov, N., and Gusev, O. (2022). Chironomid midges (Diptera) provide insights

into genome evolution in extreme environments. Curr. Opin. Insect Sci. *49*, 101–107.

5. Møbjerg, N., Halberg, K.A., Jørgensen, A., Persson, D., Bjørn, M., Ramløv, H., and Kristensen, R.M. (2011). Survival in extreme environments - on the current knowledge of adaptations in tardigrades. Acta Physiol. (Oxf). *202*, 409–420. 10.1111/j.1748-1716.2011.02252.x.

6. Møbjerg, N., and Neves, R.C. (2021). New insights into survival strategies of tardigrades. Comp. Biochem. Physiol. A. Mol. Integr. Physiol. *254*, 110890.

7. Hibshman, J.D., Clegg, J.S., and Goldstein, B. (2020). Mechanisms of Desiccation Tolerance: Themes and Variations in Brine Shrimp, Roundworms, and Tardigrades. Front. Physiol. *11*, 592016. 10.3389/fphys.2020.592016.

8. Schill, R.O., and Hengherr, S. (2018). Environmental Adaptations: Desiccation Tolerance. In Water Bears: The Biology of Tardigrades, R. O. Schill, ed. (Springer Nature Switzerland), pp. 273–294.

9. Hengherr, S., and Schill, R.O. (2018). Environmental Adaptations: Cryobiosis. In Water Bears: The Biology of Tardigrades, R. O. Schill, ed. (Springer Nature Switzerland), pp. 295–310.

10. Guidetti, R., Rizzo, A.M., Altiero, T., and Rebecchi, L. (2012). What can we learn from the toughest animals of the Earth? Water bears (tardigrades) as multicellular model organisms in order to perform scientific preparations for lunar exploration. Planet. Space Sci. *74*, 97–102. 10.1016/j.pss.2012.05.021.

11. Jönsson, K.I. (2019). Radiation Tolerance in Tardigrades : Current Knowledge and Potential Applications in Medicine. Cancers (Basel). *11*, 1333.

12. Bolus, N.E. (2001). Basic review of radiation biology and terminology. J Nucl Med Technol *29*, 67–73.

13. Beltrán-Pardo, E., Jönsson, K.I., Harms-Ringdahl, M., Haghdoost, S., and Wojcik, A. (2015). Tolerance to Gamma Radiation in the Tardigrade *Hypsibius dujardini* from Embryo to Adult Correlate Inversely with Cellular Proliferation. PLoS One *10*, e0133658. 10.5061/dryad.50r1b.

14. Steel, G.G. (1996). From targets to genes: a brief history of radiosensitivity. Phys. Med. Biol. *41*, 205–222.

15. Hashimoto, T., Horikawa, D.D., Saito, Y., Kuwahara, H., Kozuka-Hata, H., Shin-I, T.,

Minakuchi, Y., Ohishi, K., Motoyama, A., Aizu, T., et al. (2016). Extremotolerant tardigrade genome and improved radiotolerance of human cultured cells by tardigrade-unique protein. Nat. Commun. *7*, 12808. 10.1038/ncomms12808.

16. Hashimoto, T., and Kunieda, T. (2017). DNA Protection Protein, a Novel Mechanism of Radiation Tolerance: Lessons from Tardigrades. Life *7*, 26. 10.3390/life7020026.

17. Chavez, C., Cruz-Becerra, G., Fei, J., Kassavetis, G.A., and Kadonaga, J.T. (2019). The tardigrade damage suppressor protein binds to nucleosomes and protects DNA from hydroxyl radicals. Elife *8*, e47682.

18. Kamilari, M., Jørgensen, A., Schiøtt, M., and Møbjerg, N. (2019). Comparative transcriptomics suggest unique molecular adaptations within tardigrade lineages. BMC Genomics *20*, 607.

19. Jönsson, K.I., Hygum, T.L., Andersen, K.N., Clausen, L.K.B., and Møbjerg, N. (2016). Tolerance to gamma radiation in the marine heterotardigrade, *Echiniscoides sigismundi*. PLoS One *11*, e0168884. 10.1371/journal.pone.0168884.

20. Murai, Y., Yagi-Utsumi, M., Fujiwara, M., Tanaka, S., Tomita, M., Kato, K., and Arakawa, K. (2021). Multiomics study of a heterotardigrade, *Echinisicus testudo*, suggests the possibility of convergent evolution of abundant heat-soluble proteins in Tardigrada. BMC Genomics *22*, 813. 10.1186/s12864-021-08131-x.

21. Kumari, S., Rastogi, R.P., Singh, K.L., Singh, S.P., and Sinha, R.P. (2008). DNA Damage: Detection Strategies. EXCLI J. *7*, 44–62.

22. Ciccia, A., and Elledge, S.J. (2010). The DNA Damage Response: Making It Safe to Play with Knives. Mol. Cell *40*, 179–204. 10.1016/j.molcel.2010.09.019.

23. Rashi-Elkeles, S., Warnatz, H.-J., Elkon, R., Kupershtein, A., Chobod, Y., Paz, A., Amstislavskiy, V., Sultan, M., Safer, H., Nietfeld, W., et al. (2014). Parallel profiling of the transcriptome, cistrome, and epigenome in the cellular response to ionizing radiation. Sci. Signal. *7*, rs3. 10.1126/scisignal.2005032.

24. Narayanan, I.V., Paulsen, M.T., Bedi, K., Berg, N., Ljungman, E.A., Francia, S., Veloso, A., Magnuson, B., di Fagagna, F.D., Wilson, T.E., et al. (2017). Transcriptional and post-transcriptional regulation of the ionizing radiation response by ATM and p53. Sci. Rep. *7*, 43598. 10.1038/srep43598.

25. Jen, K.-Y., and Cheung, V.G. (2003). Transcriptional response of lymphoblastoid cells to

ionizing radiation. Genome Res. *13*, 2092–2100. 10.1101/gr.1240103.

26. Bouten, R.M., Dalgard, C.L., Soltis, A.R., Slaven, J.E., and Day, R.M. (2021). Transcriptomic profiling and pathway analysis of cultured human lunch microvascular endothelial cells following ionizing radiation exposure. Sci. Rep. *11*, 24214.

27. van Bergeijk, P., Heimiller, J., Uyetake, L., and Su, T.T. (2012). Genome-wide expression analysis identifies a modulator of ionizing radiation-induced p53-independent apoptosis in *Drosophila melanogaster*. PLoS One *7*, e36539. 10.1371/journal.pone.0036539.

28. Moskalev, A., Zhikrivetskaya, S., Krasnov, G., Shaposhnikov, M., Proshkina, E., Borisoglebsky, D., Danilov, A., Peregudova, D., Sharapova, I., Dobrovolskaya, E., et al. (2015). A comparison of the transcriptome of *Drosophila melanogaster* in response to entomopathogenic fungus, ionizing radiation, starvation and cold shock. BMC Genomics *16*, S8. 10.1186/1471-2164-16-S13-S8.

29. Rieger, K.E., and Chu, G. (2004). Portrait of transcriptional responses to ultraviolet and ionizing radiation in human cells. Nucleic Acids Res. *32*, 4786–4803. 10.1093/nar/gkh783.

30. Boothby, T.C., Tapia, H., Brozena, A.H., Pielak, G.J., Koshland, D., and Goldstein, B. (2017). Tardigrades use intrinsically disordered proteins to survive desiccation. Mol. Cell *65*, 975–984. 10.1016/j.molcel.2017.02.018.

31. Hibshman, J.D., Carra, S., and Goldstein, B. (2023). Tardigrade small heat shock proteins can limit desiccation-induced protein aggregation. Commun. Biol. *6*, 121.

32. Yoshida, Y., Koutsovoulos, G., Laetsch, D.R., Stevens, L., Kumar, S., Horikawa, D.D., Ishino, K., Komine, S., Kunieda, T., Tomita, M., et al. (2017). Comparative genomics of the tardigrades *Hypsibius dujardini* and *Ramazzottius varieornatus*. PLoS Biol. *15*, e2002266. 10.1371/journal.pbio.2002266.

33. Kondo, K., Kubo, T., and Kunieda, T. (2015). Suggested Involvement of PP1/PP2A Activity and De Novo Gene Expression in Anhydrobiotic Survival in a Tardigrade, Hypsibius dujardini, by Chemical Genetic Approach. PLoS One *10*, e0144803. 10.1371/journal.pone.0144803.

34. Rivera-Calzada, A., Spagnolo, L., Pearl, L.H., and Llorca, O. (2007). Structural model of full-length human Ku70–Ku80 heterodimer and its recognition of DNA and DNA-PKcs. EMBO Rep. *8*, 56–62. 10.1038/sj.embor.7400847.

35. Yu, Z., Chen, J., Ford, B.N., Brackley, M.E., and Glickman, B.W. (1999). Human DNA repair systems: An overview. Environ. Mol. Mutagen. *33*, 3–20.

36. Dizdaroglu, M. (1992). Measurement of radiation-induced damage to DNA at the molecular level. Int. J. Radiat. Biol. *61*, 175–183.

37. Demple, B., and Harrison, L. (1994). Repair of Oxidative Damage to DNA: Enzymology and Biology. Annu. Rev. Biochem. *63*, 915–948.

38. Reid, D.A., Keegan, S., Leo-Macias, A., Watanabe, G., Strande, N.T., Chang, H.H., Oksuz, B.A., Fenyo, D., Lieber, M.R., Ramsden, D.A., et al. (2015). Organization and dynamics of the nonhomologous end-joining machinery during DNA double-strand break repair. Proc. Natl. Acad. Sci. U. S. A. *112*, E2575-84. 10.1073/pnas.1420115112.

39. Wood, R.D., and Doublié, S. (2022). Genome Protection by DNA Polymerase θ. Annu. Rev. Genet. *56*, 207–228.

40. Ramsden, D.A., Carvajal-Garcia, J., and Gupta, G.P. (2022). Mechanism, cellular functions and cancer roles of polymerase-theta-mediated DNA end joining. Nat. Rev. Mol. Cell Biol. *23*, 125–140. 10.1038/s41580-021-00405-2.

41. Rodgers, K., and McVey, M. (2016). Error-prone repair of DNA double-strand breaks. J. Cell Physiol. *231*, 15–24. 10.1002/jcp.25053.

42. Anoud, M., Delagoutte, E., Helleu, Q., Brion, A., Duvernois-Berthet, E., As, M., Marques, X., Lamribet, K., Senamaud, C., Jourdren, L., et al. (2024). Comparative transcriptomics reveal a novel tardigrade specific DNA binding protein induced in response to ionizing radiation. Elife *13*, RP92621. 10.7554/eLife.92621.1.

43. Gusev, O., Nakahara, Y., Vanyagina, V., Malutina, L., Cornette, R., Sakashita, T., Hamada, N., Kikawada, T., Kobayashi, Y., and Okuda, T. (2010). Anhydrobiosis-associated nuclear DNA damage and repair in the sleeping chironomid: Linkage with radioresistance. PLoS One *5*, e14008. 10.1371/journal.pone.0014008.

44. Neumann, S., Reuner, A., Brümmer, F., and Schill, R.O. (2009). DNA damage in storage cells of anhydrobiotic tardigrades. Comp. Biochem. Physiol. A Mol. Integr. Physiol. *153*, 425–429. 10.1016/j.cbpa.2009.04.611.

45. Yoshida, Y., Satoh, T., Ota, C., Tanaka, S., Horikawa, D.D., Tomita, M., Kato, K., and Arakawa, K. (2022). Time-series transcriptomic screening of factors contributing to the cross-tolerance to UV radiation and anhydrobiosis in tardigrades. BMC Genomics *23*,

405. 10.1186/s12864-022-08642-1.

46. Bolzán, A.D., and Bianchi, M.S. (2018). DNA and chromosome damage induced by bleomycin in mammalian cells: An update. Mutat. Res. Rev. Mutat. Res. *775*, 51–62. 10.1016/j.mrrev.2018.02.003.

47. Kciuk, M., Marciniak, B., Mojzych, M., and Kontek, R. (2020). Focus on UV-induced DNA Damage and Repair—Disease Relevance and Protective Strategies. Int. J. Mol. Sci. *21*, 7264. 10.3390/ijms21197264.

48. Gross, V., Müller, M., Hehn, L., Ferstl, S., Allner, S., Dierolf, M., Achterhold, K., Mayer, G., and Pfeiffer, F. (2019). X-ray imaging of a water bear offers a new look at tardigrade internal anatomy. Zool. Lett. *5*, 14. 10.1186/s40851-019-0130-6.

49. Møbjerg, N., Jørgensen, A., Kristensen, R.M., and Neves, R.C. (2019). Morphology and Functional Anatomy. In Water Bears: The Biology of Tardigrades, pp. 57–94.

50. Kumagai, H., Kondo, K., and Kunieda, T. (2022). Application of CRISPR/Cas9 system and the preferred no-indel end-joining repair in tardigrades. Biochem. Biophys. Res. Commun. *623*, 196–201. 10.1016/j.bbrc.2022.07.060.

51. Aihara, H., Ito, Y., Kurumizaka, H., Yokoyama, S., and Shibata, T. (1999). The N-terminal domain of the human Rad51 protein binds DNA: Structure and a DNA binding surface as revealed by NMR. J. Mol. Biol. *290*, 495–504. 10.1006/jmbi.1999.2904.

52. Ghodke, H., Paudel, B.P., Lewis, J.S., Jergic, S., Gopal, K., Romero, Z.J., Wood, E.A., Woodgate, R., Cox, M.M., and van Oijen, A.M. (2019). Spatial and temporal organization of RecA in the Escherichia coli DNA-damage response. Elife *8*, e42761. 10.7554/eLife.42761.

53. Tenlen, J.R., McCaskill, S., and Goldstein, B. (2013). RNA interference can be used to disrupt gene function in tardigrades. Dev. Genes Evol. *223*, 171–181. 10.1007/s00427-012-0432-6.

54. Nussenzweig, A., Sokol, K., Burgman, P., Li, L., and Li, G.C. (1997). Hypersensitivity of Ku80-deficient cell lines and mice to DNA damage: The effects of ionizing radiation on growth, survival, and development. Proc. Natl. Acad. Sci. U. S. A. *94*, 13588–13593. 10.1073/pnas.94.25.13588.

55. Hanakahi, L.A. (2007). 2-step purification of the Ku DNA repair protein expressed in Escherichia coli. Protein Expr. Purif. *52*, 139–145.

56. Förster, F., Beisser, D., Grohme, M.A., Liang, C., Mali, B., Siegl, A.M., Engelmann, J.C., Shkumatov, A. V., Schokraie, E., Müller, T., et al. (2012). Transcriptome analysis in tardigrade species reveals specific molecular pathways for stress adaptations. Bioinform. Biol. Insights *6*, 69–96. 10.4137/BBI.S9150.

57. Horikawa, D.D., Cumbers, J., Sakakibara, I., Rogoff, D., Leuko, S., Harnoto, R., and Arakawa, K. (2013). Analysis of DNA repair and protection in the Tardigrade *Ramazzottius varieornatus* and *Hypsibius dujardini* after exposure to UVC radiation. PLoS One *8*, e64793. 10.1371/journal.pone.0064793.

58. Guidetti, R., Altiero, T., and Rebecchi, L. (2011). On dormancy strategies in tardigrades. J. Insect Physiol. *57*, 567–576. 10.1016/j.jinsphys.2011.03.003.

59. Maslowska, K.H., Makiela-Dzbenska, K., and Fijalkowska, I.J. (2019). The SOS System: A Complex and Tightly Regulated Response to DNA Damage. Environ. Mol. Mutagen. *60*, 368–384.

60. Talbert, P.B., and Henikoff, S. (2017). Histone variants on the move: substrates for chromatin dynamics. Nat. Rev. Mol. Cell Biol. *18*, 115–126. 10.1038/nrm.2016.148.

61. Zheng, Y., Li, H., Bo, X., and Chen, H. (2023). Ionizing radiation damage and repair from 3D-genomic perspective. Trends Genet. *39*, 1–4.

62. Escarcega, R.D., Patil, A.A., Meyer, M.D., Moruno-Manchon, J.F., Silvagnoli, A.D., McCullough, L.D., and Tsvetkov, A.S. (2023). The Tardigrade damage suppressor protein Dsup promotes DNA damage in neurons. Mol. Cell. Neurosci. *125*, 103826. 10.1016/j.mcn.2023.103826.

63. Yoshida, Y., Horikawa, D.D., Sakashita, T., Yokota, Y., Kobayashi, Y., Tomita, M., and Arakawa, K. (2021). RNA sequencing data for gamma radiation response in the extremotolerant tardigrade *Ramazzottius varieornatus*. Data Br. *36*, 107111. 10.1016/j.dib.2021.107111.

64. Goldstein, B. (2022). Tardigrades and their emergence as model organisms. Curr. Top. Dev. Biol. *147*, 173–198.

65. Perez-Riverol, Y., Csordas, A., Bai, J., Bernal-Llinares, M., Hewapathirana, S., Kundu, D.J., Inuganti, A., Griss, J., Mayer, G., Eisenacher, M., et al. (2019). The PRIDE database and related tools and resources in 2019: Improving support for quantification data. Nucleic Acids Res. *47*, D442–D450. 10.1093/nar/gky1106.

66. McNuff, R. (2018). Laboratory Culture of Hypsibius exemplaris. Cold Spring Harb. Protoc., 867–870. 10.1101/pdb.prot102319.

67. Gabriel, W.N., McNuff, R., Patel, S.K., Gregory, T.R., Jeck, W.R., Jones, C.D., and Goldstein, B. (2007). The tardigrade *Hypsibius dujardini*, a new model for studying the evolution of development. Dev. Biol. *312*, 545–559. 10.1016/j.ydbio.2007.09.055.

68. Denton, D., and Kumar, S. (2015). Terminal Deoxynucleotidyl Transferase (TdT)-Mediated dUTP Nick-End Labeling (TUNEL) for Detection of Apoptotic Cells in *Drosophila*. Cold Spring Harb. Protoc., 568–572. 10.1101/pdb.prot086199.

69. Schindelin, J., Arganda-Carreras, I., Frise, E., Kaynig, V., Longair, M., Pietzsch, T., Preibisch, S., Rueden, C., Saalfeld, S., Schmid, B., et al. (2012). Fiji : an open-source platform for biological-image analysis. Nat. Methods *9*, 676–682. 10.1038/NMETH.2019.

70. Carpenter, A.E., Jones, T.R., Lamprecht, M.R., Clarke, C., Kang, I.H., Friman, O., Guertin, D.A., Chang, J.H., Lindquist, R.A., Moffat, J., et al. (2006). CellProfiler : image analysis software for identifying and quantifying cell phenotypes. Genome Biol. *7*, R100. 10.1186/gb-2006-7-10-r100.

71. Liao, Y., Smyth, G.K., and Shi, W. (2013). The Subread aligner: Fast, accurate and scalable read mapping by seed-and-vote. Nucleic Acids Res. *41*, e108. 10.1093/nar/gkt214.

72. Robinson, M.D., McCarthy, D.J., and Smyth, G.K. (2010). edgeR : a Bioconductor package for differential expression analysis of digital gene expression data. Bioinformatics *26*, 139–140. 10.1093/bioinformatics/btp616.

73. Bryant, D.M., Johnson, K., Ditommaso, T., Tickle, T., Couger, M.B., Payzin-Dogru, D., Lee, T.J., Leigh, N.D., Kuo, T.-H., Davis, G.G., et al. (2017). A tissue-mapped Axolotl de novo transcriptome enables identification of limb regeneration factors. Cell Rep. *18*, 762–776.

74. Silva, J.C., Gorenstein, M. V., Li, G.Z., Vissers, J.P.C., and Geromanos, S.J. (2006). Absolute quantification of proteins by LCMSE: A virtue of parallel MS acquisition. Mol. Cell. Proteomics *5*, 144–156. 10.1074/mcp.M500230-MCP200.

75. Smith, F.W., and Goldstein, B. (2017). Segmentation in Tardigrada and diversification of segmental patterns in Panarthropoda. Arthropod Struct. Dev. *46*, 328–340. 10.1016/j.asd.2016.10.005.

76. Smith, F.W. (2018). Embryonic *in situ* Hybridization for the Tardigrade *Hypsibius exemplaris*. Cold Spring Harb. Protoc., 891–899. 10.1101/pdb.prot102350.

77. Heikes, K.L., Game, M., Smith, F.W., and Goldstein, B. (2023). The embryonic origin of primordial germ cells in the tardigrade *Hypsibius exemplaris*. Dev. Biol. *497*, 42–58.

78. Duvaud, S., Gabella, C., Lisacek, F., Stockinger, H., Ioannidis, V., and Durinx, C. (2021). Expasy, the Swiss Bioinformatics Resource Portal, as designed by its users. Nucleic Acids Res. *49*, W216–W227. 10.1093/nar/gkab225.

79. Tenlen, J.R. (2018). Microinjection of dsRNA in Tardigrades. Cold Spring Harb. Protoc., 900–904. 10.1101/pdb.prot102368.

80. R Core Team (2021). R: A language and environment for statistical computing. R Foundation for Statistical Computing, Vienna, Austria. https://www.r-project.org/.

81. Benjamini, Y., and Hochberg, Y. (1995). Controlling the False Discovery Rate: A Practical and Powerful Approach to Multiple Testing. J. R. Stat. Soc. Ser. B *57*, 289–300. 10.1111/j.2517-6161.1995.tb02031.x.

82. Hibshman, J.D., and Goldstein, B. (2021). LEA motifs promote desiccation tolerance in vivo. BMC Biol. *19*, 263. 10.1186/s12915-021-01176-0.

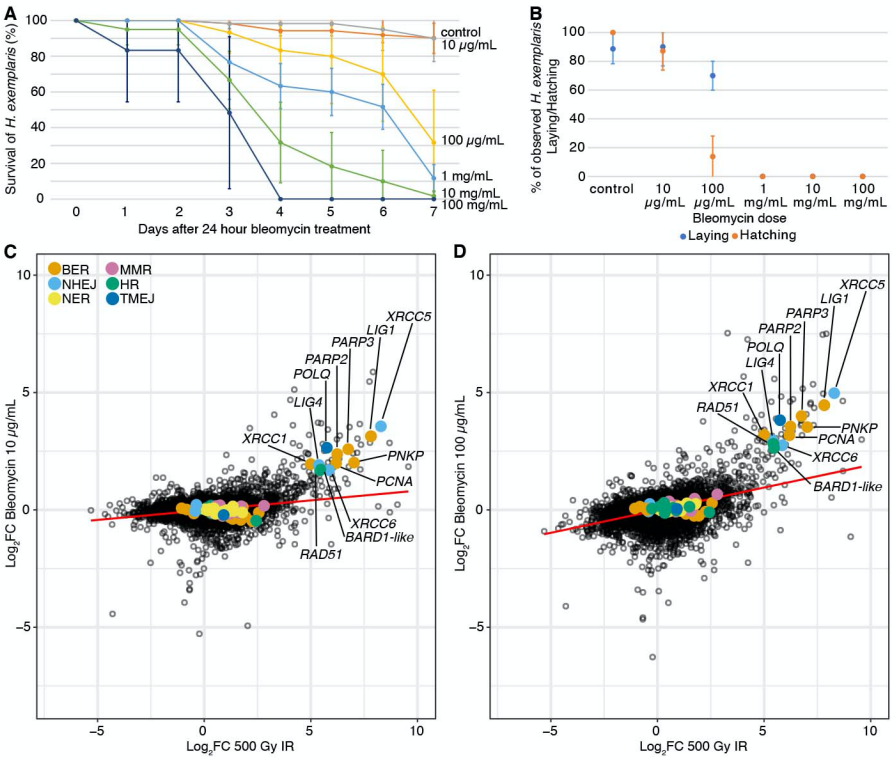

Figure S1: Bleomycin serves as a useful radiomimetic in *H. exemplaris* and induces a transcriptional response similar to ionizing radiation, related to Figure 3. (**A**) Plot showing mean survival (+/- standard deviation (sd)) over 7 days after treatment with the designated dose of Bleomycin for 24 hours (n=60 for each treatment group except for the control (n=54) and 100 µg/mL (n=50), see Data S1 for detailed n by trial). (**B**) Plot showing the percent of observed animals (+/- sd) that laid clutches (laying, dark blue) and the percent of laying animals that had viable clutches (hatching, orange) after treatment with the designated dose of Bleomycin for 24 hours (n for laying is the same as survival above, n for hatching is as follows: control=48, 10 µg/mL=49, 100 µg/mL=30, and 0 for 1 mg/mL, 10 mg/mL, and 100 mg/mL, see Data S1 for detailed n by trial). (**C** and **D**) Plots showing Log_2FC of transcripts in response to 10 µg/mL (**C**) and 100 µg/mL (**D**) Bleomycin plotted against the Log_2FC of transcripts in response to 500 Gy IR. R-squared values for the trendlines are 0.0962 and 0.2312, respectively (Pearson correlation test, p<.0001). Colors are the same as in Figure 2. LIG1 is colored as BER (orange), but also functions in TMEJ (dark blue). See also Data S1F.

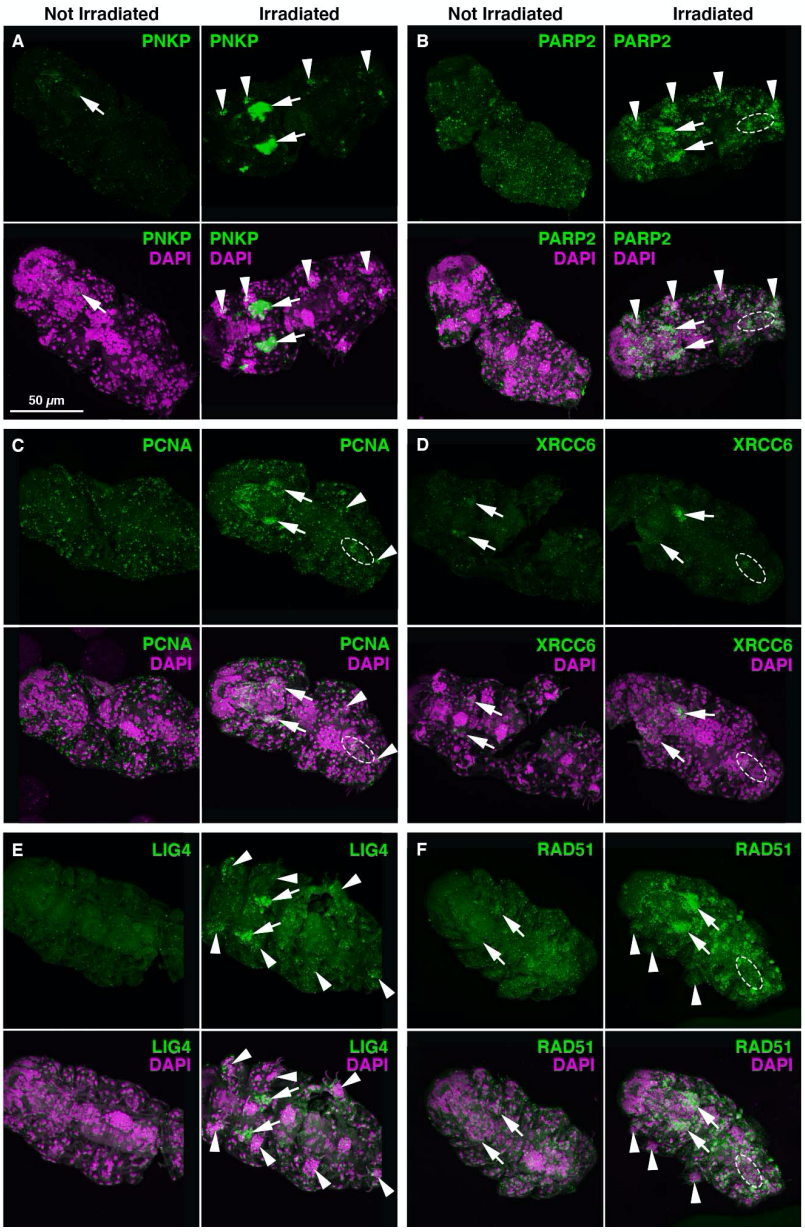

Figure S2. Tissue-specific enrichment of tardigrade DNA repair transcripts following ionizing radiation exposure, related to Figure 4. (**A-F**) Representative images of *in situ* hybridization for DNA repair transcripts with and without exposure to 100 Gy ionizing radiation. Exposure and contrast were adjusted here to visualize regions of most intense signal. Expression in stylet glands (arrows), claw glands (arrowheads), and hindgut (dashed outlines) is indicated where seen. Transcripts encoding members of the BER (**A-C**), NHEJ (**D-E**), and HR (**F**) pathways are represented. Scale bar in A applies to all images. Anterior is to the left. Orientation of each image is as follows: dorsal up: (**A,E**) not irradiated, (**B,D**) irradiated, (**C**), and (**F**); ventral up: (**A,E**) irradiated, (**B,D**) not irradiated.

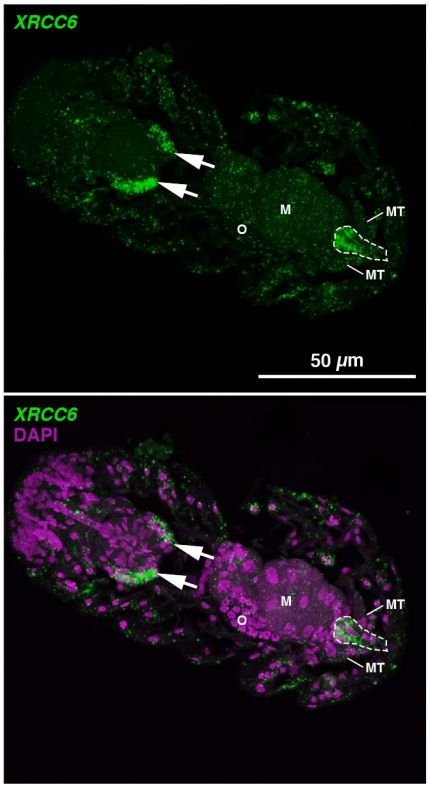

Figure S3. Enrichment of DNA repair transcript in hindgut of tardigrades following ionizing radiation, related to Figure 4. Maximum projection of optical sections containing hindgut expression of *XRCC6* to demonstrate hindgut location and identification. Expression in stylet glands (arrows) and hindgut (dashed outlines) is indicated where seen. Other landmark structures have been indicated as follows: O (Ovary), M (Midgut), and MT (Malpighian Tubules). Anterior is to the left, dorsal is up.

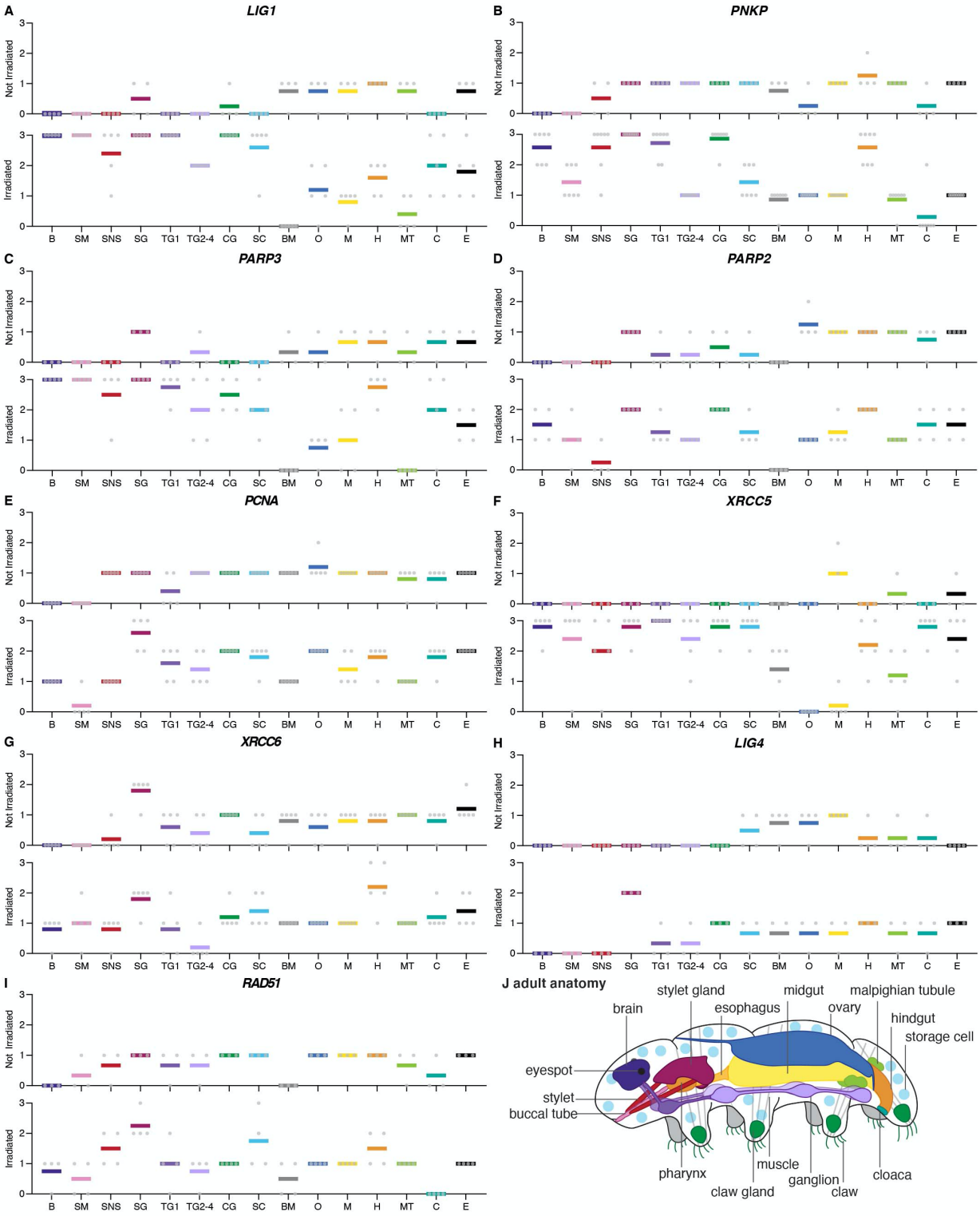

Figure S4. *in situ* hybridization for DNA repair transcripts reveals transcript accumulation in many tissues with some tissue-specific enrichment, related to Figure 4. (**A-I**) Tissue-specific enrichment profiles for DNA repair transcripts with and without exposure to 100 Gy IR. Tissue abbreviations are as follows: B (Brain), SM (Stylet Muscle), SNS (Stomodeal Nervous

System, associated with stylet), SG (Stylet Gland), TG1 (Trunk Ganglion segment 1), TG2-4 (Trunk Ganglion segments 2-4), CG (Claw Gland), SC (Storage Cells, free-floating throughout the body cavity), BM (Body Muscle), O (Ovary), M (Midgut), H (Hindgut), MT (Malpighian Tubules), C (Cloaca), and E (Epidermis). Tissues were scored from 0 (no observed expression) to 3 (high expression) (see Materials and Methods for details on expression scoring). Tissue identification based on morphological analysis and informed by [S1]. Transcripts encoding members of the BER, TMEJ, NHEJ, and HR pathways are all represented. (**J**) Schematic of a lateral view of an adult tardigrade with landmark structures indicated (adapted from [S2]). Some anatomical features including longitudinal muscles, SM, and SNS are not shown in this diagram. The buccal tube and stylet are colored pink and fuchsia, respectively as their location within *H. exemplaris* anatomy correlates with the locations of SM and SNS, respectively. See also Data S1G.

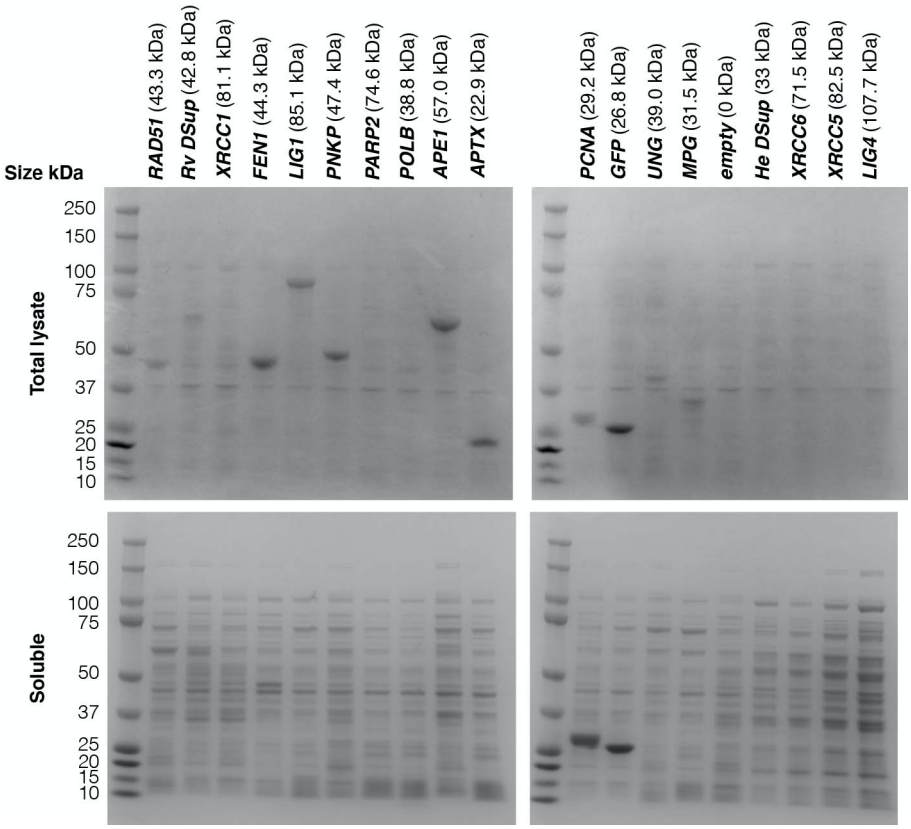

Figure S5. Bacterial expression of tardigrade DNA repair proteins, related to Figure 5. Protein gels showing levels of expression (top) and solubility (bottom) of tardigrade proteins heterologously expressed in *E. coli*.

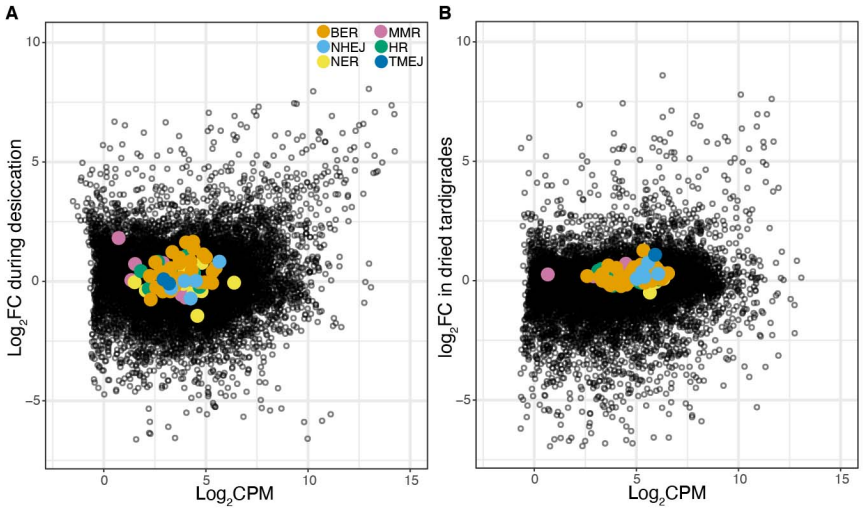

Figure S6. Transcriptional response of DNA repair genes to desiccation, related to Figures 2 and 3. (A and B) MA plots displaying Log_2FC of *H. exemplaris* transcripts during desiccation (A) and in dried tardigrades (B). Some BER and MMR transcripts are enriched slightly during desiccation (A) and a TMEJ transcript is enriched in dried animals (B). Original data from [S3] and [S4] (A) and [S5] (B). Legend in A also applies to B. See also Data S1H.

DNA Repair Pathway	Gene ID	logFC	logCPM	PValue	FDR	Protein
N/A	BV898_10457	13.47446	9.7397723	0	0	Hypothetical Protein: No conserved domains, tardigrade-specific
NHEJ	**BV898_01166**	**8.3019188**	**12.811847**	**0**	**0**	**XRCC5 (Ku80)**
BER/TMEJ	**BV898_18082**	**7.8223532**	**12.813553**	**0**	**0**	**DNA Lig1**
N/A	BV898_03941	7.3494104	8.394104	0	0	Hypothetical Protein - Histone H4 Domain
N/A	BV898_10478	7.1855765	10.834309	0	0	Core histone macro-H2A.1
BER	**BV898_14774**	**7.0250053**	**9.9533286**	**0**	**0**	**PNKP**
BER	**BV898_07590**	**6.7555331**	**11.95287**	**0**	**0**	**PARP3**
N/A	BV898_17031	6.7823053	9.0346048	7.12E-320	1.27E-316	Mitochondrial chaperone BCS1
N/A	BV898_07145	6.3337674	7.9604761	3.40E-314	5.41E-311	XRCC6 (Ku70) partial
N/A	BV898_09662	6.7606824	7.871877	2.01E-310	2.88E-307	Hypothetical Protein: No conserved domains, tardigrade-specific
BER	**BV898_08059**	**6.2385156**	**10.658468**	**3.26E-304**	**4.24E-301**	**PARP2**
N/A	BV898_10564	9.5751369	6.3851308	2.05E-291	2.44E-288	Protein phosphatase 1B
N/A	BV898_16497	6.7294928	8.2529798	1.86E-280	2.05E-277	Hypothetical Protein - Ring and WWE domains
BER	**BV898_09437**	**6.1884444**	**9.0754975**	**3.31E-265**	**3.38E-262**	**PCNA**
NHEJ	**BV898_18536**	**5.3786796**	**9.7114364**	**5.27E-251**	**5.02E-248**	**DNA Lig4**

Table S1. Top 15 Significantly enriched transcripts following exposure to 500 Gy ionizing radiation, related to Figure 2. Transcripts that encode members of DNA repair pathways are in bold.

Gene ID	Protein	0 Gy Rep 1 log_2 TPM	0 Gy Rep 2 log_2 TPM	0 Gy Rep 3 log_2 TPM	500 Gy Rep 1 log_2 TPM	500 Gy Rep 2 log_2 TPM	500 Gy Rep 3 log_2 TPM	0 Gy Mean log_2 TPM	500 Gy Mean log_2 TPM
BV898_08387	Hypothetical Protein: No conserved domains	15.30	15.23	15.17	15.32	15.27	15.16	15.23	15.25
BV898_03848	**Elongation factor 1-alpha**	**13.85**	**13.91**	**13.49**	**13.67**	**13.68**	**13.84**	**13.75**	**13.73**
BV898_04261	28S ribosomal RNA	12.79	12.99	12.75	12.71	13.41	14.39	12.84	13.50
BV898_16263	SAHS 33020	13.54	13.69	13.80	13.39	13.32	13.01	13.68	13.24
BV898_02877	**Actin, cytoplasmic 1**	**14.06**	**14.18**	**13.71**	**13.09**	**13.11**	**13.34**	**13.98**	**13.18**
BV898_01166	XRCC5 (Ku80)	4.96	4.88	4.87	13.03	13.01	13.15	4.90	13.06
BV898_07590	PARP3	6.29	6.25	6.12	12.84	12.83	12.88	6.22	12.85
BV898_17177	putative Ovochymase-1	12.98	12.87	12.87	12.84	12.82	12.85	12.91	12.84
BV898_01079	Hypothetical Protein: No conserved domains, tardigrade-specific	11.91	11.95	11.64	12.69	12.77	12.72	11.83	12.73
BV898_18082	DNA Lig1	5.03	5.04	4.91	12.68	12.63	12.74	4.99	12.68
BV898_13380	Hypothetical Protein: No conserved domains, tardigrade-specific	12.78	12.76	12.24	12.50	12.51	12.64	12.59	12.55
BV898_10202	Hypothetical Protein: No conserved domains, tardigrade-specific	12.39	12.30	12.16	12.52	12.52	12.59	12.28	12.54
BV898_02951	Hypothetical Protein: PTZ00491 super family	8.19	8.36	8.34	12.49	12.43	12.26	8.29	12.39
BV898_09382	Cathepsin L1	12.32	12.28	12.39	12.35	12.30	12.29	12.33	12.31
BV898_09692	Hypothetical Protein: No	7.99	8.13	7.78	12.28	12.28	11.92	7.97	12.16

conserved domains, tardigrade-specific				

Table S2. Top 15 most highly represented transcripts after 500 Gy ionizing radiation, related to Figure 2. Ordered from highest-to-lowest mean log_2TPM after 500 Gy IR exposure. Genes encoding housekeeping proteins are in bold.

DNA Repair Pathway	Gene ID	logFC	logCPM	PValue	FDR	Protein
HR	BV898_05956	5.4671337	10.057325	3.18E-232	2.39E-229	BARD1-like
HR	BV898_00321	5.4364268	8.8928117	4.90E-225	3.34E-222	Rad51
HR	BV898_20143	5.3117773	7.7081581	1.76E-224	1.14E-221	BARD1-like C-terminus domain
BER	BV898_11662	5.0021574	9.6958034	1.87E-222	1.17E-219	XRCC1
TMEJ	BV898_12022	5.7518622	10.02558	1.15E-219	6.51E-217	DNA Pol Theta
NHEJ	BV898_13167	5.8565378	8.8210533	3.04E-209	1.61E-206	XRCC6 (Ku70)

Table S3. Additional significantly enriched DNA repair transcripts with $Log_2FC > 3$ following exposure to 500 Gy ionizing radiation, related to Figure 2.

DNA Repair Pathway	Gene ID	logFC	logCPM	PValue	FDR	Protein
BER	BV898_07584	2.559571496	2.690908549	2.16E-26	5.00E-25	POLE
BER	BV898_14389	2.259704982	2.658781627	5.67E-19	7.65E-18	POLE
BER	BV898_00699	1.938523112	3.946204532	1.45E-16	1.57E-15	POLE
BER	BV898_11940	1.812787291	5.175856368	7.77E-41	3.84E-39	NEI1
BER	BV898_05905	1.715659906	0.849748331	7.85E-06	2.30E-05	POLE
BER	BV898_09130	1.622126568	2.934751658	1.49E-14	1.32E-13	POLE
BER	BV898_12106	1.403846148	3.289002334	3.94E-12	2.69E-11	MPG
BER	BV898_07011	1.339077393	4.583430605	4.13E-08	1.70E-07	PCNA2
BER	BV898_19255	1.217464256	2.896466295	5.83E-09	2.72E-08	APTX
BER	BV898_05497	0.942180716	1.435580686	1.89E-04	4.49E-04	XRCC2
BER	BV898_17297	0.931547307	3.827553195	4.14E-07	1.47E-06	APE1
BER	BV898_06939	0.901606578	4.346174316	1.73E-07	6.50E-07	TDP1
BER	BV898_17296	0.85395349	4.231937117	4.92E-06	1.49E-05	UNG
BER	BV898_16090	0.407334092	3.284999309	0.029377591	0.04575854	XRCC3
BER	BV898_11887	0.311979756	5.336223394	0.024269471	0.038579262	FEN1
BER	BV898_18106	0.290024277	5.663595701	0.054423861	0.079743248	PARP1
BER	BV898_12491	0.198459441	4.045586689	0.239072056	0.297178116	POLB
BER	BV898_13647	-0.486211099	2.261781292	0.04769684	0.070881291	APTX
BER	BV898_00690	-0.50290121	3.136987623	0.007063355	0.012528325	OGG1
BER	BV898_01320	-0.825151897	3.954118904	6.23E-06	1.86E-05	TDG
BER	BV898_01675	-1.058763936	3.218067581	2.13E-07	7.86E-07	PARP2
BER/NER	BV898_02288	1.098576718	4.328746335	2.40E-11	1.48E-10	POLD
BER/NER	BV898_07442	1.053458803	5.689481845	7.73E-12	5.10E-11	POLD
BER/NER	BV898_06679	0.45201805	5.188409411	0.002699767	0.005216826	POLD
BER/NER	BV898_18581	0.249721779	4.311852127	0.133859217	0.178093015	POLD
HR	BV898_09463	2.439463408	1.87645143	2.39E-20	3.68E-19	RAD51-like protein 3
HR	BV898_04885	1.502820055	3.342528438	8.82E-14	7.23E-13	SLX1
HR	BV898_07655	0.883977031	2.996584345	1.16E-05	3.30E-05	SLX4
HR	BV898_09156	0.733526628	4.427052093	3.56E-06	1.10E-05	EME1
HR	BV898_04385	0.341189952	3.365318181	0.135974764	0.180521485	MUS81
HR	BV898_04742	0.311300214	2.319764499	0.153886739	0.201091605	RAD51-like protein 4
HR	BV898_09974	0.118763681	5.949688494	0.399458552	0.463781721	RAD50
HR	BV898_01799	-0.260551856	5.696031878	0.053950569	0.079163288	MRE11
MMR	BV898_01929	2.805657967	6.9121655	7.77E-73	9.11E-71	RFC
MMR	BV898_18044	1.741017443	4.259958877	7.48E-21	1.20E-19	PMS2
MMR	BV898_01995	1.67386983	3.885875031	9.45E-18	1.14E-16	RFC
MMR	BV898_09367	1.580671088	2.8170678	1.99E-07	7.40E-07	MLH1
MMR	BV898_01879	1.38186033	4.203953871	3.68E-10	1.98E-09	MSH2

MMR	BV898_12462	1.190593667	4.10363447	8.52E-11	4.96E-10	RFC
MMR	BV898_18005	1.179099402	3.571739886	1.23E-06	4.07E-06	EXO1
MMR	BV898_02250	0.863632609	3.805178833	8.94E-07	3.02E-06	RFC
MMR	BV898_08111	0.743496098	2.936863103	0.002435904	0.004735745	MSH5
MMR	BV898_14807	0.691382776	4.035805732	6.65E-05	0.000169228	RFC
MMR	BV898_19257	0.552872561	2.8725312	0.022954226	0.036622821	MSH4
MMR	BV898_18042	0.545024276	2.319286138	0.012507116	0.021188334	PMS2
MMR	BV898_00821	0.358160365	5.254667196	0.044602273	0.066691283	MSH6
NER	BV898_09884	1.78717657	2.807520788	1.19E-17	1.43E-16	CDK7
NER	BV898_04619	1.382825885	4.411488478	1.03E-18	1.36E-17	XPA
NER	BV898_16920	1.345978434	4.656851752	1.38E-20	2.16E-19	ERCC2
NER	BV898_19171	1.314854205	5.958875498	2.55E-20	3.92E-19	DDB
NER	BV898_04343	1.197584605	5.426072695	6.43E-13	4.80E-12	DDB
NER	BV898_03001	1.060128151	6.21861266	9.95E-16	1.00E-14	RAD23
NER	BV898_15865	0.997414808	3.811851229	7.36E-08	2.91E-07	GTF2H4/TFIIH4
NER/TMEJ	BV898_04720	0.913429269	2.569835142	3.16E-05	8.44E-05	ERCC1
NER	BV898_07753	0.882817479	3.738124237	1.15E-05	0.0000328	GTF2H2/TFIIH2
NER	BV898_09677	0.644767709	5.819792523	2.82E-06	8.90E-06	ERCC3
NER	BV898_08303	0.533807963	3.260013836	0.006410445	0.011491405	GTF2H3/TFIIH3
NER	BV898_12642	0.451973114	4.3168946	0.016891475	0.027824796	ERCC5
NER	BV898_12642	0.451973114	4.3168946	0.016891475	0.027824796	ERCC5
NER	BV898_17903	0.173792439	4.947762788	0.210278876	0.265399623	CETN2
NER	BV898_09502	0.147141597	4.689256598	0.324535323	0.387002151	GTF2H1/TFIIH1
NER	BV898_04735	0.139990253	7.036893483	0.282814819	0.343435143	RAD23
NER	BV898_15700	0.029460608	5.302953833	0.847945705	0.877386134	ERCC5
NHEJ	BV898_14444	-0.365288742	6.25029778	0.00821843	0.014416265	DNA PKCS
NHEJ	BV898_01836	-0.419071587	4.396791518	0.006299683	0.01131554	NHEJ1/XLF

Table S4. DNA repair transcripts with Log_2FC <3 following exposure to 500 Gy ionizing radiation, related to Figure 2.

Primer Name	Sequence	Amplicon Length	Purpose
He_LIG1_p_F1	ATCCATCAACAGCCGCAAGA	809	*in situ* hybridization probe
He_LIG1_p_R1	**TAATACGACTCACTATAG**CCGTCACAGCTTCCAATCCT		
He_PNKP_p_F1	TTGCACGTGTACAATCCCGA	649	*in situ* hybridization probe
He_PNKP_p_R1	**TAATACGACTCACTATAG**CCTGAGAGGCAGATGCCAAA		
He_PARP3_p_F1	CCCCGGGACGTATAAACAGG	805	*in situ* hybridization probe
He_PARP3_p_R1	**TAATACGACTCACTATAG**ACCGTACTTGATGTCGCAGG		
He_PARP2_p_F1	GTGATGCGGGATTTCGAAGC	818	*in situ* hybridization probe
He_PARP2_p_R1	**TAATACGACTCACTATAG**AAGCAGTAGTTGGCGCTCTT		
He_PCNA_p_F2	ATCAAGGATCTGTTGGGCGA	711	*in situ* hybridization probe
He_PCNA_p_R2	**TAATACGACTCACTATAG**GTTGATCTTCGGAGCCAGGT		
He_XRCC5_p_F2	TACCAGCCGAACGATGAAG	756	*in situ* hybridization probe
He_XRCC5_p_R2	**TAATACGACTCACTATAG**GACCGAACTTGTCTTAGCCT		
He_XRCC5_i_F1	**TAATACGACTCACTATAG**GGGTAAAAGCGTCTCACCGA	759	dsRNA template amplification
He_XRCC5_i_R1	**TAATACGACTCACTATAG**TTCCCATCCAACAAGGGAGC		
He_XRCC6_p_F1	ATCAGCGGATGATGACGACC	659	*in situ* hybridization probe
He_XRCC6_p_R1	**TAATACGACTCACTATAG**AGTCATCGGCAAAGGGGAAG		
He_LIG4_p_F1	ACTGGGAGCCAAAAGGATCG	867	*in situ* hybridization probe
He_LIG4_p_R1	**TAATACGACTCACTATAG**TAGCTGTCAAGCACCCACTG		
He_RAD51_p_F1	TACTCAACCGGTGGTGAAGC	864	*in situ* hybridization probe
He_RAD51_p_R1	**TAATACGACTCACTATAG**CGATTCTCCCCCTTGCCTTT		
GFP_i_F1	**TAATACGACTCACTATAG**ATGAGTAAAGGAGAAGAACTTTTCACTGG	717	dsRNA template amplification
GFP_i_R1	**TAATACGACTCACTATAG**TTATTTGTATAGTTCATCCATGCCATGTGT		

Table S5. Primers used in this study, related to STAR Methods. Bold: T7 promoter sequence

SUPPLEMENTAL REFERENCES

S1. Gross, V., Müller, M., Hehn, L., Ferstl, S., Allner, S., Dierolf, M., Achterhold, K., Mayer, G., and Pfeiffer, F. (2019). X-ray imaging of a water bear offers a new look at tardigrade internal anatomy. Zool. Lett. *5*, 14. 10.1186/s40851-019-0130-6.

S2. Goldstein, B. (2022). Tardigrades and their emergence as model organisms. Curr. Top. Dev. Biol. *147*, 173–198.

S3. Boothby, T.C., Tapia, H., Brozena, A.H., Pielak, G.J., Koshland, D., and Goldstein, B. (2017). Tardigrades use intrinsically disordered proteins to survive desiccation. Mol. Cell *65*, 975–984. 10.1016/j.molcel.2017.02.018.

S4. Hibshman, J.D., Carra, S., and Goldstein, B. (2023). Tardigrade small heat shock proteins can limit desiccation-induced protein aggregation. Commun. Biol. *6*, 121.

S5. Yoshida, Y., Koutsovoulos, G., Laetsch, D.R., Stevens, L., Kumar, S., Horikawa, D.D., Ishino, K., Komine, S., Kunieda, T., Tomita, M., et al. (2017). Comparative genomics of the tardigrades Hypsibius dujardini and Ramazzottius varieornatus. PLoS Biol. *15*, e2002266. 10.1371/journal.pbio.2002266.